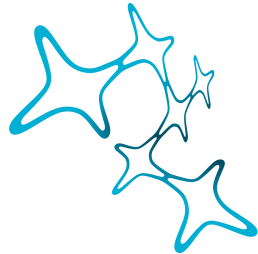


LUDWIG-MAXIMILIANS-UNIVERSITÄT
MÜNCHEN
FACULTY OF BIOLOGY, COMPUTATIONAL NEUROSCIENCE



Graduate School of
Systemic Neurosciences
LMU Munich

MASTER'S THESIS

**Computational Simulation of
Time Perception**

Katharina M BRACHER

Supervision: Dr. Kay THURLEY
Prof. Dr. Andreas HERZ

Contents

1	Introduction	3
1.1	Behavioral Effects in Magnitude Estimation	3
1.2	Time Estimation via Predictive Timing	4
1.3	A Dynamical Systems Approach	5
2	Model Description	6
2.1	Basic Circuit	7
2.2	Update Mechanism and Experiment Procedure	8
3	Parameters in Accordance with Error Minimization	12
3.1	Behaviorally Plausible Slopes	13
3.2	Model Regime for Error-Minimized Behavior	13
4	Comparison of Intermediate and High Input Regime	15
4.1	Comparison of Dynamics	16
4.2	Experiment Simulation in the High Input Regime	16
4.3	Error-Minimizing Parameters in the High Input Regime	17
4.4	Comparison of Experiment Simulations	18
5	General Underestimation	19
5.1	Delay Period Influences Reproductions	20
5.2	Adjusted Experiment Simulation	20
6	Influence of External Variability on Behavior	22
6.1	Effects of Stimulus Statistics in Real Behavior	22
6.2	Optimality Predicts Regression Effect and Range Effect	23
6.3	Optimality Predicts no Effect of Variance on Behavior	24
6.4	Comparison of Behavioral Output of Model to Real Data	25
7	Discussion	27
7.1	Representation of Stimulus Statistics	28
7.2	Scales of Timing	30
7.3	Integration into Classical and Bayesian Framework	31
	Supplements	32
	References	44

Abstract

Time reproduction experiments are a useful approach to the study of sensory processing because a relationship is established between external events and their internal perception. In such experiments, behavioral responses are characterized by specific biases such as the central tendency or regression effect, i.e. the overestimation of small time intervals and the underestimation of large ones. Sensory information is combined expectations based on prior knowledge to minimize errors arising from noise in the environment and neural signal.

To flexibly adjust behavior to the time actions, the brain is thought to dynamically change patterns of neural activity. The speed of neural dynamics is adjusted according to the reproduced time interval. This has been well described with a dynamical systems approach, adjusting the initial conditions and external inputs of the system Paton and Buonomano 2018, Issa et al. 2020, Zhou et al. 2022. Here we investigate a neural circuit model that has been proposed recently to explain various timing behaviors, including the reproduction of time intervals (Egger, Le, et al. 2020).

The input to the circuit controls at which speed the readout unit increases its activity and therefore scales its responses such that a threshold is reached at different times. During the presentation of the stimulus interval, the circuit predicts the to-be-reproduced duration. From the mismatch between this prediction and the actual stimulus duration, an error signal is derived, according to which the input and consequently the speed is adjusted for the subsequent reproduction.

We found robust conditions for realistic time reproduction experiments that are consistent with characteristic behavioral effects. A crucial parameter is the weight with which the input to the circuit is adjusted to balance the mismatch between the predicted interval and the stimulus duration. Adjusting this weight in accordance with error minimization, leads to putting more weight on the prior experience for longer stimuli, which naturally entail more uncertainty, and is thus biological plausible.

1 Introduction

Animals are capable of producing complex and flexible behaviors that often rely on the interplay of motor and sensory systems. Timing is critical for many of these sensorimotor functions, ensuring the ability to anticipate and coordinate interactions with the environment. Sensory and motor timing in the millisecond range is particularly important, as this timescale includes temporal cues for vocalization as well as fine motor coordination. Despite its importance, there is no sensory organ responsible for time perception, which means that time perception must be generated internally by extracting information from sensory inputs. Although time is pervasive in animal behavior, it is elusive and difficult to study and the neural implementation that allows the brain to perceive and internally perform complex temporal computations remains unknown. Nevertheless, the mechanism of timing might provide powerful insights into general mechanisms of cognition and neural computations (Issa et al. 2020).

Magnitude estimation is a useful approach to explore sensory processing because it involves establishing a relationship between external events and their internal perception by, for example, evaluating or reproducing a time interval. However, externally-derived inputs are subject to noise arising from the variability of the environment. In addition, noise arising from neural representations of the input affects the perception of time. A variety of experimental studies have found characteristic behavioral effects across sensory modalities in magnitude reproduction experiments that might arise to minimize errors in the presence of noise (Petzschner, Glasauer, et al. 2015).

1.1 Behavioral Effects in Magnitude Estimation

The most striking observation in stimulus reproduction is regression to the mean of stimuli, in other words, small stimuli are overestimated whereas large stimuli are underestimated (*regression effect*). This effect intensifies for ranges with larger stimuli (*range effect*). Also, the standard deviation of estimates increases monotonically for larger stimuli (*scalar variability*). Finally, the recent history of stimuli presentations influences the current stimuli estimation (*sequential effects*). All effects mentioned above are displayed in Fig. 1. Modality-independence of these effects suggests the existence of a common underlying principle or processing mechanisms, that would explain e.g. an optimal strategy for unreliable judgments due to noise. Minimizing errors in judgment can

be achieved by integrating prior experience with immediate sensory input, and is therefore often described with Bayesian models. In Bayesian models, sensory information is represented by a likelihood function and is combined with prior experience that together result in biased estimates. However, it has not been shown how the brain would implement such behavior.

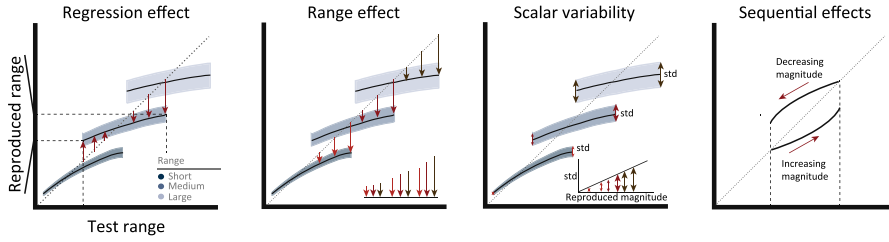


Figure 1: **Behavioral effects.** *Regression effect*: in a distribution of stimuli large stimuli are underestimated, and small stimuli are overestimated which results in a regression to the mean of the range. *Range effect*: the regression to the mean gets more pronounced for ranges that comprise larger stimuli. *Scalar variability*: the standard deviation of the reproduced magnitude grows linearly with larger estimates. *Sequential effects*: the history presented stimuli (e.g. ascending or descending order) has an influence on the reproduced magnitude. Adapted from Petzschner, Glasauer, et al. 2015.

1.2 Time Estimation via Predictive Timing

Experiments, in which subjects have to measure and reproduce time intervals, can be used to study how the brain integrates expectations with current sensory input in order to achieve correct timing. Time reproduction is usually accomplished by at least one presentation of the time interval e.g. between two external events (sensory timing), and a reproduction period that is terminated by the subject's movement initiation (motor timing). In both epochs elapsed time needs to be estimated, the difference lies in the termination of the interval. In sensory timing, the time interval is terminated by an external event, while in the motor timing, the completion is internally generated and executed by a motor command.

Time between two events can be measured in an absolute or predictive manner. In the case of absolute timing, time can be continuously estimated from an output that results from integration of ticks from a central clock. The rate at which activity increases does not depend on the time interval. In contrast, for predictive timing a fixed state is reached at the end of the time interval,

by adjusting the rate of a process according to the anticipated time. Recently, evidence of predictive timing has emerged suggesting, that the CNS makes use of predictive signaling mechanisms, allowing the animal to contemplate sensory consequences of actions (Meirhaeghe et al. 2021, Egger, Remington, et al. 2019).

Predictive coding is a framework, in which the brain is predicting its upcoming states and refining these predictions through error signals (Ficco et al. 2021, Huang and Rao 2011, Rao and Ballard 1999). Intrinsic neural representations of motor actions are used as predictor of sensory consequences. If there is a mismatch in predicted and actual sensory feedback, an internal model is updated by the error signal (Straka et al. 2018, Clark 2013, Bubic et al. 2010). The internal model can include a prior to integrate expectations into the time estimate. Based on predictions and expectations, flexible control of neural mechanisms is required to measure and produce time intervals. This raises the question of how flexible control over brain dynamics can be achieved?

1.3 A Dynamical Systems Approach

A brain area that has been associated with timing behavior is the medial pre-frontal cortex (MFC) (Wang et al. 2018, Emmons et al. 2017, Genovesio et al. 2006, Lewis et al. 2004, Shima and Tanji 2000). In time reproduction experiments, the activity of individual cells in the MFC shows heterogeneous response profiles, many of which are temporally scaled according to the produced time interval (Henke, Bunk, et al. 2021, Sohn et al. 2019, Remington et al. 2018, Wang et al. 2018). Indeed, time can be encoded predicatively relative to the mean of time intervals by temporal scaling activity. Scaling is a phenomenon that is consistent at the population level, when activity is displayed in a low-dimensional state space. In the state space, the activity of all neurons is represented over time by a so-called neural trajectory (Cueva et al. 2020). It has been shown that for sensory timing, the population activity evolves along a common trajectory, whereas in motor timing, trajectories scale in speed to reach a common terminal state, that triggers an action (Henke, Bunk, et al. 2021, Meirhaeghe et al. 2021, Sohn et al. 2019, Wang et al. 2018, Murakami et al. 2014, Mita et al. 2009). Experiments have shown a causal link for population dynamics encoding time. Cooling the MFC down, slowed population dynamics down, resulting in longer time estimates (Xu et al. 2014). Therefore, the brain dynamically changes patterns of neural activity to flexibly adjust behavior to time actions, where flexible motor timing can be achieved by controlling the speed of neural dynamics (Tsao

et al. 2022, Sohn et al. 2019, Remington et al. 2018, Wang et al. 2018).

Data indicates that neural trajectories reflect the internal estimate of a time interval and are influenced by a prior. Experiments with multiple, consecutive measurement periods showed a sequential update of the estimate, providing evidence for a predictive process with an error signal extracted from the previous epoch to correct the speed of the neural trajectory. Wang et al. 2018 proposed a potential neural mechanism for speed control by flexibly adjusting the effective time constant of a network. In fact, the population activity reflects an interval-dependent speed command that is updated based on a mismatch between predicted and actual interval in measurement epochs (Egger, Remington, et al. 2019, Wang et al. 2018).

Building on these findings, Remington et al. 2018 showed that flexible control of behavior in interval reproduction can be understood in terms of a dynamical system that is characterized by the initial state and an external input. In a two-neuron-model, that is well known for modeling decision-making (Roxin and Ledberg 2008), the input level can be used to adapt the effective time constant of the system. Based on that mechanism, Egger, Le, et al. 2020 developed an extended circuit model for sensorimotor timing. The model was used in interval reproduction tasks and fitted to human data that exhibited classical effects of magnitude estimation. However, different time intervals were presented separately and not in a random sequence as in classical time reproduction experiments.

By applying the circuit model to simulations that reflect more realistic conditions of time reproduction experiments, this work addresses the questions which effects in behavior can be explained by the model. We demonstrated that in realistic experiment simulations, classical effects of magnitude estimation are captured by the model, that itself is only based on principles found in brain data. Following this result, the effects of external variability of time intervals are examined. The predictions of the model are evaluated and compared to data of time reproduction experiments with gerbils and humans.

2 Model Description

Flexible speed control can be achieved by a simple model consisting of three units, u, v, y that represent population activity.

2.1 Basic Circuit

The dynamics of u , v , and y are defined as follows:

$$\begin{aligned}\tau \frac{du}{dt} &= -u + \theta(W_{uI}I - W_{uv}v + \eta_u), \\ \tau \frac{dv}{dt} &= -v + \theta(W_{vI}I - W_{vu}u + \eta_v), \\ \tau \frac{dy}{dt} &= -y + W_{yu}u - W_{yv}v + \eta_y.\end{aligned}\tag{1}$$

Two units, u and v , receive a tonic symmetric input I ($W_{uI} = W_{vI} = 6$) and are mutually inhibiting each other ($W_{uv} = W_{vu} = 6$). The inputs to u and v are governed by a sigmoid activation function $\theta(x) = \frac{1}{1+exp(-x)}$. The output unit y receives excitatory input from u and inhibitory input from v ($W_{yu} = W_{yv} = 1$) which results in a ramp-like activity of y . All three units have a time constant $\tau = 100$ ms. Stochastic synaptic inputs are modeled as independent white noise η_u, η_v, η_y with standard deviation σ . Initial conditions of u, v and y have been optimized for in Egger, Le, et al. 2020 and are set to $u_0 = 0.7, v_0 = 0.2, y_0 = 0.5$ (Fig. 2a)

Depending on the input I , the system shows different dynamics. For low levels of I ($0 < I < 0.5$) the system has three fixed points (two stable, one unstable at $u = v$) and y ramps up faster the higher input I . For intermediate values of I ($0.5 < I < 1$) the system still shows three fixed points of the same sort as in the low input regime (Fig. 2b) but y ramps up with a slope that is inversely proportional to the input I (y ramps up slower the higher input I , see Fig. 2c). For high I ($1 < I$) the system has one stable fixed point (at $u = v$) and y ramps down faster for higher I . Thus, the speed at which the output y evolves can be controlled by the input I (Fig. 2d) and determines the time interval after which y reaches a fixed threshold y_{th} . In interval reproduction experiments, reaching a threshold y_{th} can be understood as movement initiation time, which can be controlled for by adjusting I . In this report, the intermediate input regime is explored: higher inputs result in a shallower slope of y , such that the threshold y_{th} is reached after a longer time interval.

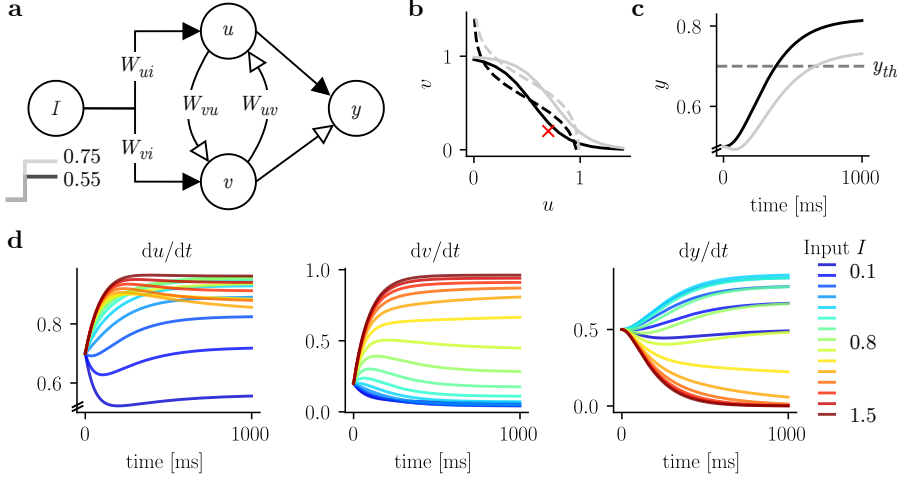


Figure 2: Basic circuit and input regimes. (a) u and v share a common input I . The input is governed by weights W_{uI} and W_{vI} . The two units have reciprocal inhibitory connections, with weights W_{uv} and W_{vu} that determine the inhibitory strength. Both project to the output unit y with an excitatory connection from u and an inhibitory connection from v . Excitatory and inhibitory connections are shown by filled and open arrows, respectively. (b) The control of the speed in y can be analyzed in the phase plane of u and v . The u (dashed) and v nullcline (solid) is shifted when the input is increased from $I = 0.65$ (black) to $I = 0.75$ (gray). In the intermediate regime, the systems shows two stable and one unstable fixed point. The red cross indicates the initial conditions for the dynamics in (c). Depending on I , with the same initial conditions, the system evolves faster or slower to the stable fixed point. (c) Dynamics of y for intermediate regime with input $I = 0.75$ in gray and $I = 0.65$ in black. There is an inverse relation of input strength and slope. With higher input, the threshold at 0.7 (dashed line) is reached after a longer time interval. (d) Dynamics of u, v, y for inputs from $0.1 \leq I \leq 1.5$ are shown. Initial conditions are set to $u_0 = 0.7, v_0 = 0.2, y_0 = 0.5$. With these initial conditions and values of $I \geq 0.5$, the relation of steady state activity of y (and slope to reach the steady state) is inverse to I (intermediate and high I regime). For values $I \leq 1$ the activity of y ramps down (yellow corresponds to $I = 1$). For $I < 0.5$ the steady state (slope) is smaller the smaller I (low I regime, dark blue).

2.2 Update Mechanism and Experiment Procedure

Basic interval reproduction experiments can be designed with only two epochs: a measurement epoch that has the duration of the stimulus interval and a reproduction epoch that starts immediately after the measurement epoch (Fig. 3b). The basic circuit described above is modified to perform interval reproduction (see Figure 3a for schematic of modified circuit). The relation of input I with the slope of the ramping activity of y is used in combination with a fixed threshold y_{th} . By adding an update mechanism that flexibly adjusts I , the threshold crossing of y can be delayed or moved to earlier times. This way, measuring and reproducing an interval is done predictively, by adjusting the slope of the ramp such that the output reaches the threshold after the intended time. In

in the model the measurement epoch is fixed to the stimulus interval t_s , and the reproduction epoch ends, when y reaches the fixed threshold y_{th} from below. The time from the end of the measurement epoch until the threshold-crossing of y yields the reproduced time interval t_r that is aimed to equal the stimulus interval t_s (Fig. 3c).

The following update mechanism of I is based on the intermediate input regime, that shows an inverse relation of I to the slope of y (Fig. 2b). The error signal is determined at the end of the measurement epoch and is composed of the difference of y to the threshold y_{th} . If the threshold y_{th} is not reached during the measurement epoch, the slope has to be adjusted, such that y ramps up faster to reach the threshold at exactly the time of the stimulus interval. For a steeper slope, I is reduced. If y crossed the threshold before the measurement epoch ends, so is above y_{th} by the end of the stimulus interval, the slope needs to be reduced in order to reach the threshold at a later time in the reproduction. For a shallower slope, I is increased (Fig. 3c). I is adjusted according to the error $(y - y_{\text{th}})$, weighted by a memory parameter K right at the end of the measurement epoch

$$\tau \frac{dI}{dt} = sK(y - y_{\text{th}}) . \quad (2)$$

The update of I is only active for a pulse between the measurement and reproduction epoch ($s = 1$) and inactive for all other times ($s = 0$). Further, u and v receive a transient input pulse I_r to reset the dynamics for the subsequent epoch (Fig. 3c)

$$\begin{aligned} \tau \frac{du}{dt} &= -u + \theta(W_{uI}I - W_{uv}v + \eta_u - I_r) , \\ \tau \frac{dv}{dt} &= -v + \theta(W_{vI}I - W_{vu}u + \eta_v + I_r) . \end{aligned} \quad (3)$$

Resetting the dynamics after the reproduction epoch enables the model to simulate an arbitrary number of stimulus intervals. Before a new stimulus presentation there is a delay period: at the beginning of an experiment with a sequence of stimuli there is an initial interval with the initial values of u, v, y and an initial input I_0 (Fig. 3c). This initial interval allows the model to get closer to steady-state before the stimulus presentation starts. Reproductions that do not reach the threshold in a certain time span or too early are classified as timeout

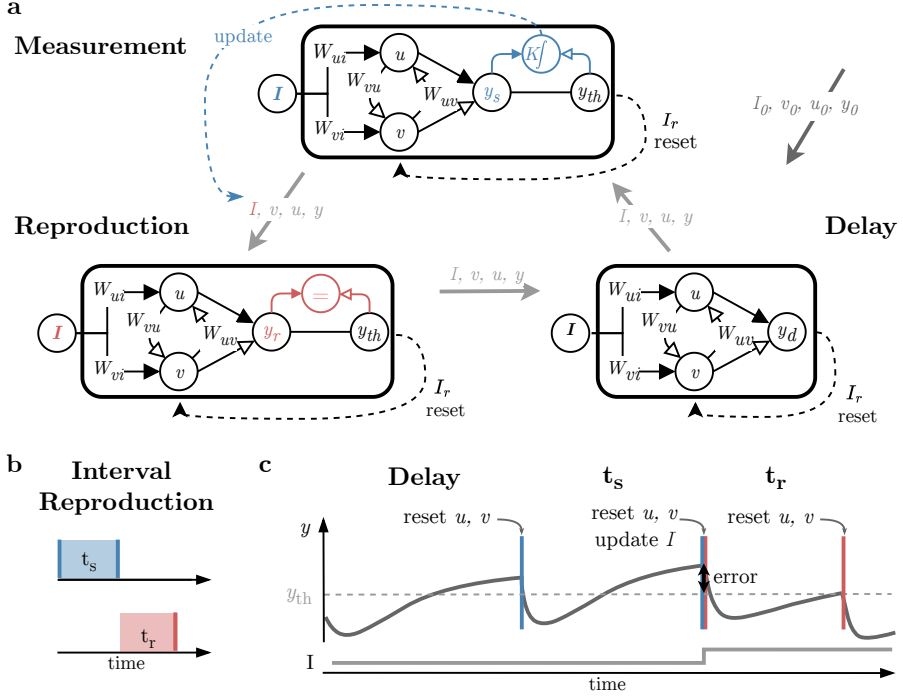


Figure 3: Extended circuit for experiment simulation. (a) The circuits for measurement, reproduction and delay epoch are displayed. All circuits comprise the same basic structure with different additional elements that are unique for the epoch. Initial values of u, v, y and I are fed into the delay circuit for the duration of the initial interval. u and v are reset with a transient input I_r before end values of u, v, y and I are transferred to the measurement circuit as new initial conditions. After the duration of the stimulus interval, the difference between y and the threshold y_{th} is used with the memory parameter K to update I together with another reset of u and v . The values are transferred with all other variables to the reproduction circuit. The reproduction epoch ends when y reaches the threshold y_{th} from below. Before the presentation of another stimulus interval, there is again a delay period with no update of I . The reset mechanism enables the model to simulate an arbitrary number of stimulus intervals. Adapted from Egger, Le, et al. 2020. (b) Interval reproduction experiment with stimulus interval t_s (blue) and reproduction t_r (red). (c) Schematic of one trial. After a delay epoch, u and v are reset. The measurement epoch lasts for the duration of the stimulus interval t_s . y should reach the threshold y_{th} (dashed line) at exactly the time the stimulus interval ends. The threshold was crossed well before the end of the interval and at the end of the measurement epoch, the error in y_m to the threshold y_{th} is used to update I . To reach the threshold at a later time, I is increased, which reduces the slope of y in the reproduction epoch. After the reset of u and y and the update of I the reproduction ends when y reaches the threshold. The time after the reset and update until the threshold crossing denotes the reproduced interval t_r .

trial.

To simulate variability in the reproductions as it is found in real data, noise is added to u , v and y in the implementation. In data, a monotonic increase of the standard deviation of reproductions is found (*scalar variability*). If noise levels in the model are too high ($\sigma > 0.2$) the standard deviation of reproductions is not growing monotonically with σ (Egger, Le, et al. 2020). For all simulations, σ was set to 0.02, which results in a realistic coefficient of variation of 0.1 (Supplementary Fig. 1b, c). In Figure 4a five example trials and the activity of u , v , y and I are depicted. In the full simulation, 500 stimuli randomly chosen from a stimulus distribution were presented. The uniform distribution of time intervals is denoted as stimulus range. The stimulus range consisted of seven stimuli ranging from 400-700 ms (4b).

The experiment simulation results in a distribution of reproduced time intervals for each stimulus and a distribution of inputs that drive the activity of y in the reproduction (Fig. 4c). Taking the mean over the distribution of reproduced time intervals for each stimulus allows for the investigation of effects in the behavioral results (Fig. 4d).

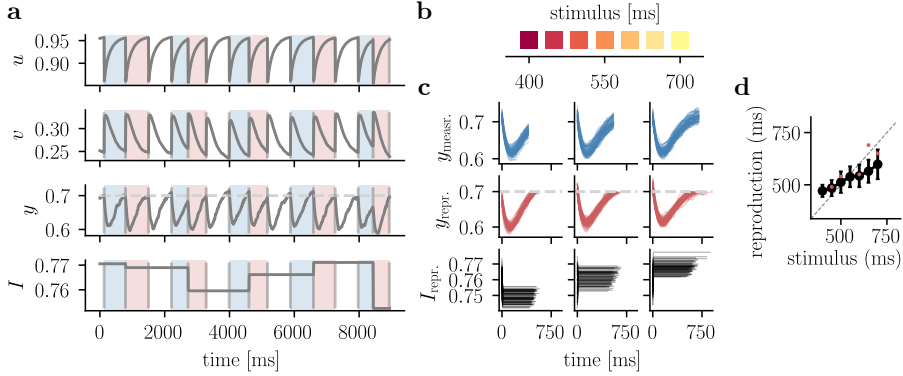


Figure 4: Experiment description. (a) The dynamics of u , v , y and I are displayed over time for five consecutive example trials (650, 500, 600, 700, 450 ms) of an experiment simulation with 500 trials. Stimulus presentation and reproduction epochs are highlighted in blue and red, respectively. Before new stimuli presentations, there is a 700 ms delay period (white). Initial values for the experiment simulation are set to $u_0 = 0.7$, $v_0 = 0.2$, $y_0 = 0.5$, $I_0 = 0.8$. The added noise is set to $\sigma = 0.02$ and the memory parameter to $K = 5$. The threshold is set to $y_{\text{th}} = 0.7$ (dashed line). Reproduced times are 690, 540, 550, 650, 490 ms. (b) For the experiment, simulation time intervals were randomly drawn from a discrete, uniform stimulus distribution. The range of time intervals contained stimuli from 400 to 700 ms with steps of 50 ms. (c) The measurement (upper) and reproduction (middle) epoch of y and input for reproduction (lower) are shown for the full experiment, sorted according to stimulus interval. Shown are trials for stimuli of 400, 550 and 700 ms (depicted above). (d) Mean reproduction and standard deviation (black) across trials for each stimulus interval of the experiment stimulation shown (c). If the mean lies on the identity line (dashed line), reproduction time corresponds to the stimulus interval on average. Red dots show the reproductions of the example trials shown in (a).

3 Parameters in Accordance with Error Minimization

We asked whether the behavioral effects observed in real data (Fig. 1) could be reproduced by experiments with the circuit model, which itself is based on the scaling phenomenon found in brain data. A crucial value to adapt was the memory parameter K , since this parameter defines the weight with which the input is adjusted to compensate for the discrepancy between the predicted interval and the stimulus duration. Another parameter that had to be considered is the time constant τ , which affects how fast y behaves in response to the input. Therefore, τ can be interpreted as a biophysical parameter of the model that describes the rate of a population. In contrast to Egger, Le, et al. 2020, parameters such as the initial values, especially I_0 did not need to be adjusted in advance. This is because the input will have settled after the first one or two trials and will not be affected by the initial values thereafter. In the following, the threshold was

set to 0.7, but smaller and larger thresholds were tested as well. For evaluating effects in behavior, two stimulus ranges were used in simulations, denoted as short and long range. The short range contained seven stimuli ranging from 400-700 ms. The long range also contained seven stimuli that were shifted up by 300 ms compared to the short range, ranging from 700-1000 ms.

3.1 Behaviorally Plausible Slopes

The regression effect in behavior can be quantified by the slope that results from a linear regression between the stimuli and the reproductions. Biological plausible slopes lie around 0.83 for the short and 0.73 for the long range. Interestingly, this is the case in across time domains, regardless of whether the short and long range are situated in the millisecond or second domain. (Thurley and Schild 2018, Jazayeri and Shadlen 2010). The slopes of behavioral results for multiple combinations of the update parameter K and the time constant τ were determined. In broad parameter regimes, the reproductions show a regression to the mean, as indicated by a slope smaller than 1. For fixed τ , the regression increases as K increases, since more weight is given to the current update, and consequently less reliance is placed on the prior. The model also produced biological plausible slopes for different time constants (Fig. 5a), where K must be adjusted depending on the stimulus range and time constant. To produce plausible slopes, K takes on smaller values for the long range, putting less weight on the update compared to the short range.

3.2 Model Regime for Error-Minimized Behavior

Can behavioral effects of magnitude estimation also be achieved by adjusting K and τ in accordance with error minimization? To find such optimized parameters, the mean squared error was minimized, which is defined as the sum of the squared bias and variance of the mean reproductions (Supplementary Eq. 1). This error reflects the trade-off between bias and variance, with bias error indicating over-assumptions (underfitting) and the variance error indicating variability across reproduction and thus sensitivity to noise (overfitting). For larger time constants τ , the optimized update parameter K increases. Values of K that minimize errors are smaller for the long range compared to the short range for all τ , as already found for values of K that result in plausible slopes. The corresponding time constant τ for the overall minimum of the MSE differ between the two stimulus ranges. For the short stimulus range, $\tau^* = 120$ ms

and $K^* = 11$ yields an overall minimum, whereas $\tau^* = 200$ ms, $K^* = 20$ yields a overall minimum for the long range. Assuming the same rate time constant across experiments, we had to find a shared τ for both the short and long range. Consequently, a time constant between the optima was chosen, considering the overlap with biological plausible slopes. Only with a time constant of 130 ms, optimal K coincided with biological plausible slopes in both ranges. With a time constant of $\tau = 130$, $K^* = 13$ for the short and $K^* = 10$ for the long range (Fig. 5b, Supplementary Fig. 3a, b). Behavioral results with error-minimizing parameters show a regression to the mean with a stronger regression for the long range (slope of 0.73) compared to the short range (slope of 0.77) (Fig. 5c). For dynamics of y for single trials over the course of the experiment, see Supplementary Fig. 2. Adjusting K in accordance with error minimization, leads to putting more weight on the prior experience for longer stimuli, which naturally entail more uncertainty, and is thus biological plausible. The model produces behavior that shows the regression and the range effect. Yet, the slope for the small range lies below the biological plausible slopes found in data. The standard variation of reproductions increases linearly (scalar variability), the mean coefficient of variation (CV) for the short range is 0.09, for the long range 0.11 (Fig. 5c). No range effect can be observed when minimizing the error in reproductions based on the squared bias or the variance instead of the MSE. The relation of stronger weighting of the prior for the long range due to decreased K is not apparent for either error metrics (Supplementary Fig. 3c, d).

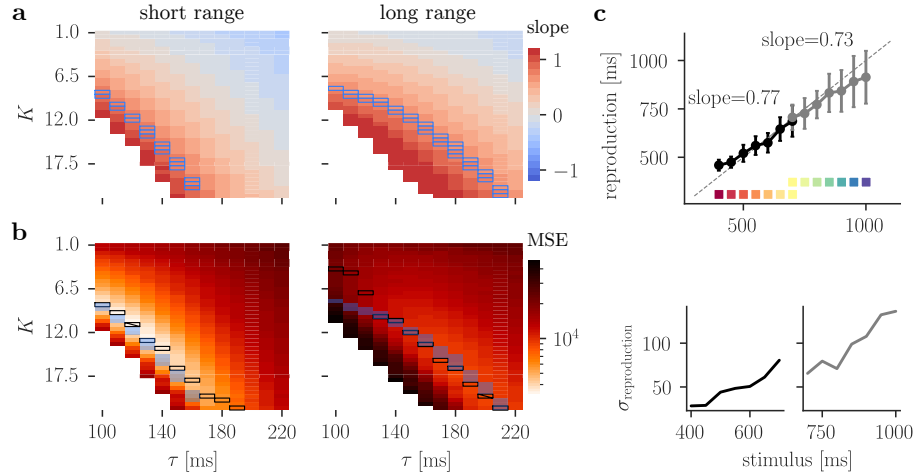


Figure 5: Behavioral effects and parameter optimization. (a) Simulations with 500 trials for each pair of memory parameter K and time constant τ at noise level $\sigma = 0.02$. Simulations were performed with stimuli chosen from the short (left) or long range (right). Color scale represents the slope of the linear fit between stimuli and reproductions. A slope of 1 on the identity line corresponds to perfect reproduction of the stimuli. Behaviorally plausible slopes are encircled in blue and lie around 0.83 for the short and 0.73 for the long range. Empty space corresponds to simulations, that exceeded the number of timeout trials and were thus excluded from analysis. (b) Optimization of the weight given to the update K for different time constants τ at noise level $\sigma = 0.02$. Color scale represents the MSE for an experiment stimulation with 500 trials for each pair of K and τ . Stimuli were either chosen from the short (left) or the long stimulus range. The minimal error for each τ is encircled in black and minimal error across all τ is additionally crossed. Parameter combinations that result in behaviorally plausible slopes (a) are shaded in blue. (c) Top: Mean reproductions for simulation with 500 trials for each stimulation with the short (black) and long (gray) stimulus range. The value of K is optimized for a time constant of $\tau = 130$ ms. For the simulation with short stimulus range K_* was 13, with the long stimulus range optimal K_* was 10. The slope is the result of a linear regression between stimuli and reproductions. Inset: For experiment simulations two stimuli ranges were used. The short range contained stimuli from 400 to 700 ms, the long range contained stimuli from 700 to 1000 ms. Bottom: Standard deviation of reproductions for each stimulus for the short and long range from the simulation in (c).

4 Comparison of Intermediate and High Input Regime

There are differences between the intermediate and high input regimes in terms of fixed points and dynamics. Nevertheless, simulations of time reproduction experiments are possible in both regimes. In the following, simulations in the high input regime are performed and compared with those in the intermediate input regime.

4.1 Comparison of Dynamics

While in the intermediate input regime three fixed points emerge in the phase plane (two stable and one unstable), in the high input regime the fixed points merge to a single one. The single fixed point is located at comparatively high activity of u and v (Fig. 6b, d). This affects the dynamics of u and v such that y ramps up in instead of down as observed in the intermediate regime. Increasing I results in steeper activity of y in the high input regime. This is reversed compared to the intermediate input regime, where an increased I leads to flatter slopes in Y (Fig. 6a, c).

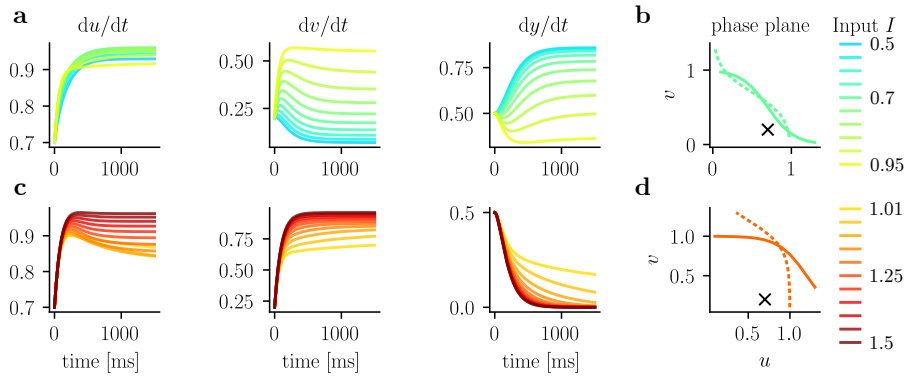


Figure 6: Comparison of dynamics in the intermediate and high input regime. (a) Evolution of u , v and y over time for different inputs from 0.5 to 0.95 in the intermediate input regime. Activity in y shows a ramping-up activity. The activity of y evolves to different steady states depending on the input. (b) The phase plane in the intermediate input regime shows two stable and one unstable fixed point. The nullclines of u (dashed) and v (solid) are shifted to higher activities when the input I is increased. The plot shows nullclines corresponding to an input of 0.7 and the black marker indicates the initial condition of dynamics in (a). (c) Same as (a) for the high input regime with inputs from 1.01 to 1.5. Activity in y shows a ramping-down activity, converging to 0 independent of input. (d) Same as (b) for high input regime. The phase plane in the high input regime shows one stable fixed point. The nullclines of u (dashed) and v (solid) are shifted to lower activities when the input I is increased. The plot shows nullclines corresponding to an input of 1.2 and the black marker indicates the initial condition of dynamics in (c).

4.2 Experiment Simulation in the High Input Regime

To simulate time reproduction experiments in the high input regime, the following changes must be made. The threshold was set to a value lower than 0 (e.g. 0.1) and initial I was increased to a value above 1 ($I_0 = 1.02$). The reset

impulse after each epoch had to be stronger by a factor of 10 and with opposite sign to bring the activity in y back to a higher level.

$$\begin{aligned}\tau \frac{du}{dt} &= -u + \theta(W_{uI}I - W_{uv}v + \eta_u + 10 * I_r) , \\ \tau \frac{dv}{dt} &= -v + \theta(W_{vI}I - W_{vu}v + \eta_v - 10 * I_r) .\end{aligned}\quad (4)$$

There is no need to change the update mechanism, even though the relation of the input I and the slope is reversed. This is because y approaches the threshold from above and not from below, so the relation of y and y_{th} is reversed and the update of I is correct.

The noise was set to the same value as in simulations in the intermediate regime ($\sigma = 0.02$). The standard deviations increased linearly. For increasing σ the standard deviation drops slightly and then plateaus for σ larger than 0.1. The CV has similar values as in the intermediate regime with 0.13 for the short and 0.12 for the long range for a σ of 0.02 (Supplementary Fig. 4a). An example of the experiment dynamics for four consecutive stimuli is displayed in Fig. 7a.

4.3 Error-Minimizing Parameters in the High Input Regime

Just as for the intermediate input regime, optimized parameter K and τ were found that minimize the MSE of reproductions. Again, the model is able to produce biologically plausible slopes for most time constants. Across all τ larger 40 ms, optimal K is smaller for the long range compared to the short range. The MSE is minimal for $\tau^* = 60$ ms for both the short and the long range, with $K^* = 4$ and $K^* = 2.5$ for the short and the long range, respectively. Optimal τ^* and K^* result in a biologically plausible slope only for the long range (slope of 0.68). For the short range the slope is too flat (slope of 0.74). Behavioral results of experiment simulation with error-minimizing parameters show a regression to the mean. In contrast to the intermediate input regime, standard deviations of the reproductions do not grow linearly in the long range (Fig. 7b). For dynamics of y over the whole experiment see Supplementary Fig. 5.

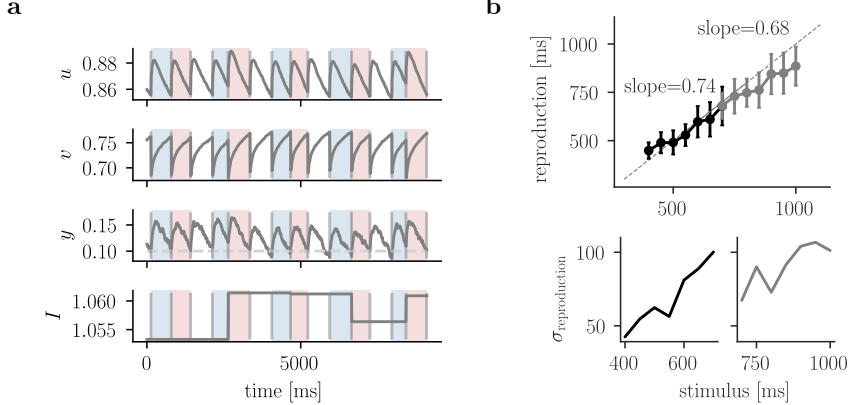


Figure 7: Experiment Simulation in the High Input Regime. (a) Activity of u, v, y and I for five example stimulus intervals of 650, 500, 600, 700, 450 ms. Stimulus presentation and reproduction epochs are highlighted in blue and red, respectively. The delay period between trials is shown in white. Initial values are set to $u_0 = 0.8, v_0 = 0.6, y_0 = 0.1, I_0 = 1.04$ and the threshold y_{th} is set to 0.1. (b) Top: Mean reproductions for simulation with 500 trials for each stimulation with the short (black) and long (gray) stimulus range. The value of K is optimized to minimize errors in reproductions for a time constant of $\tau = 60$ ms. For the simulation with short stimulus range optimal K was 4, with the long stimulus range optimal K was 2.5. The slope is the result of a linear regression between stimuli and reproductions. Bottom: Standard deviation of reproductions for each stimulus for the short and long range from the simulation in (b).

4.4 Comparison of Experiment Simulations

The results of simulations with optimal parameter combinations were used to compare the simulations in the intermediate and high input regimes. Their behavioral results are displayed in Fig. 5c for the intermediate and Fig. 7b for the high input regime. The mean input I for each stimulus shows an almost linear increase (or decrease for the high input regime) within a range. The increase (or decrease) is shallower for the long range due to the lower K^* used in the simulation (Fig. 8b, d). The maximum and minimum input I during the simulation for the short or the long range were used to examine the most distant nullclines of u and v in the phase plane (Fig. 8a, c). In the intermediate regime, the difference between maximal and minimal I is larger and the nullclines are also farther apart.

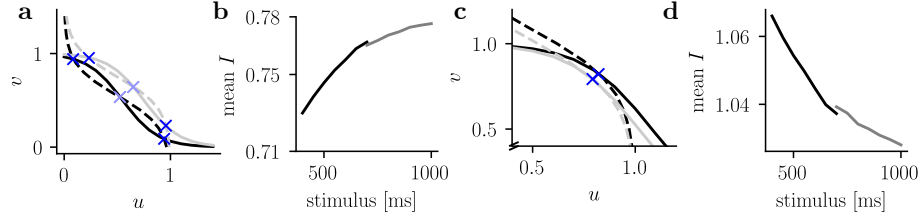


Figure 8: **Comparison of experiment simulations.** (a) The phase plane in the intermediate input regime shows two stable (blue) and one unstable (light blue) fixed point. The nullclines of u (dashed) and v (solid) are displayed. Black and gray nullclines correspond to an input of 0.71 and 0.79, respectively, which corresponds to the maximal and minimal input in the experiment simulation for the short and long range in Fig. 5c. (b) Mean input during the reproduction epoch for each stimulus of the short (black) and long (gray) range for the experiment simulation in the intermediate input regime with optimized parameters from Fig. 5c. (c) The phase plane in the high input regime shows one stable (blue) fixed point. The nullclines of u (dashed) and v (solid) are displayed. Black and gray nullclines correspond to an input of 1.081 and 1.017, respectively, which corresponds to the maximal and minimal input in the experiment simulation for both the short and long range in Fig. 7b. (d) Same as (b) for the experiment simulation in the high input regime with optimized parameters from Fig. 7b.

5 General Underestimation

For a regression to the mean the indifference point of a linear regression between stimuli and reproductions should correspond to the mean of the stimulus range (550 ms for the short and 850 ms for the long range). The indifference point (for behavioral results in Fig. 5c) is 595 ms for the short range and 710 ms for the long range. Thus, in the long range stimuli are in general underestimated. The same is the case for the high input regime (7b). What is the reason for the general underestimation of larger inputs? It is not uncommon for stimuli in larger ranges to be generally underestimated in magnitude estimation across time domains. Time reproduction experiments with gerbils and humans show a general underestimation across ranges (Fig. 11a, Henke, Flanagin, et al. 2022). The cause has not yet been researched and could be due to many reasons ranging from lapsing attention to impatience. It is necessary to investigate whether the underestimation in the model's behavioral output is caused by the regime in which the model operates, or whether it is a phenomenon that arises from optimal choice of parameters. Possible parameters of the model that could influence the behavior are the delay period between trials, the fixed threshold and the common time constant between stimulus ranges.

5.1 Delay Period Influences Reproductions

The simulations were performed with a common time constant τ that was set between the optimal τ^* for the short and long range, respectively. General underestimation in simulations with the long range can be compensated by increasing the time constant towards the optimum of the long range. However, this causes a general overestimation in the simulation with the short range (Supplementary Fig. 3b). Thus, a common time constant τ contributes to the under- and overestimation of stimuli, when it's too far from the range's optimum. But even at the optimum, simulations show a slight general underestimation in the long range. Hence, there are several causes for this problem.

Another observation is that for both the long and short range, the best reproductions were obtained for stimuli near to 700 ms. Following this observation, we simulated an experiment with a stimulus range that was situated around 700 ms (550, 600, 650, 700, 750, 800, 850 ms). The mean of 700 ms corresponds to the maximum of the short range and the minimum of the long range, and also complies with the length of the fixed delay period between trials. In Fig. 9a the behavioral results show regression to the mean with a slope of 0.82 and an indifference point of 657 ms. When setting the delay period at the maximum of the long range instead (1000 ms), a general overestimation of stimuli from the short range occurs (Supplementary Fig. 6c). This led to the assumption that a delay period too far from the range's mean leads to under- or overestimation. A comparatively short delay period compared to the mean of stimuli leads to distorted updates, because y cannot reach threshold value in the short time period with mean I . After resetting, the following measurement period is started from lower values in y . Setting the delay period equal to the mean of the short or long range eradicates general underestimation (Supplementary Fig. 6a, b). In the high input regime, adapting the delay period does not resolve the general underestimation. Thus, only the intermediate input regime is used in the following analysis.

5.2 Adjusted Experiment Simulation

The previous analysis showed, that there are two main problems that caused distorted stimulus reproductions. First, a common time constant between experiments with different ranges skews the reproductions. Second, is a hyperparameter of the experimental design affecting the reproductions. The delay period between trials should not influence reproductions. Since the time con-

stant in the model can be interpreted as a rate time constant, it is justifiable to adapt it between experiment with different stimulus ranges. This would correspond to a firing rate adjustment in the population to an experimental setting. In a biological system, an inhibitory population could scale the rate time constant according to the stimulus statistics. Furthermore, the model needs to be adjusted to take into account the impact of the delay period on the reproductions. Setting the delay time to the mean of the stimulus range used in the simulation doesn't make sense from a design perspective. It should be possible to choose the delay period between trials arbitrarily and independently of the stimulus range. Similarly, the delay period could be chosen long enough to allow the system to evolve to a steady state. However, this would mean that the delay time cannot be chosen independently. Another way to solve the problem of the delay epoch, is to neglect the delay in the simulation of the experiment (Fig. 9b). The reproduction period always ends when the threshold y_{th} is met. If the measurement period of the subsequent trial follows directly after it, it always starts at the same value of y . This does not necessarily mean, that the experimental design is limited. When simulating experiments that include a delay period between trials or even between measurement and reproduction epoch, it can be assumed that information is stored in the system until the beginning of the next epoch. In neural networks, it has been shown that the timing information in the state space can be held over a delay time (Bi and Zhou 2020). Neglecting the delay epoch in combination with independent τ^* for each range leads to characteristic effect and biologically plausible slopes (Fig. 9c). Solutions that incorporate a delay period into the simulation itself would require model adjustments. Either the reset is changed from an impulse to a fixed reset value, or the input is updated separately during the delay epoch based on an error to always reach the threshold.

Unless otherwise specified, error-minimizing τ^* and a delay of 0 ms are used for each stimulus range in following simulations. The regime of I remains similar to previous simulations with delay and common τ . There is an overlap in I and K is no longer comparable due to separate τ between different ranges (Fig. 10b).

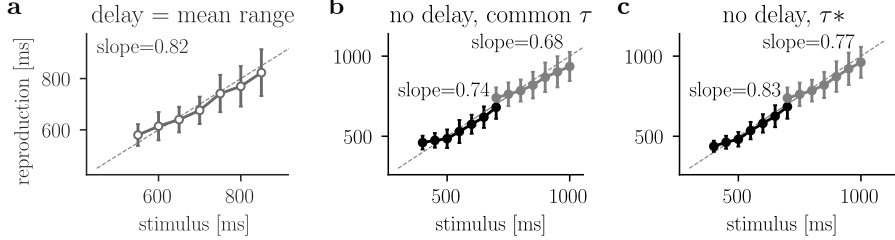


Figure 9: **Behavioral results with altered delay.** (a) Behavioral results of an experiment simulation with the previously utilized delay of 700 ms. The stimulus range that was used to sample stimuli from has a mean equal to the delay of 700 ms. The time constant and update parameter were both optimized based on the MSE ($\tau = 170$ ms, $K = 17.5$). Other parameters like threshold and initial values were not changed. (b) The delay period was set to 0 ms in simulations with the short and long range (black and gray, respectively). The time constant was set to 165 ms, which corresponds to the mean of the optimal τ for the short (130 ms) and long (200 ms) range. For $\tau = 165$ ms, the update parameter K was optimized (short range $K = 21$, long range $K = 13$). Note different axes of figures in (a) and (b). (c) Same as (b) but with independent, optimal time constant. For the short range $\tau^* = 130$, $K = 14$ and for the long range $\tau^* = 200$, $K = 20$.

6 Influence of External Variability on Behavior

Regression to the mean depends on the discrimination abilities of the individual subject. In the model, this is reflected by internal noise σ . In addition, variability of the environment affects the behavior, which is captured by the statistics of stimuli over the course of an experiment. When internal noise is fixed, the external variability can be modified independently. The effect of external variability on the update parameter can be investigated by modifying the mean or the variance of stimuli.

6.1 Effects of Stimulus Statistics in Real Behavior

With larger time intervals, internal estimates get noisier and regression of reproductions gets stronger. This is well described by the *range effect* across species (Cicchini et al. 2012, Henke, Bunk, et al. 2021, Henke, Flanagin, et al. 2022, Sohn et al. 2019). Besides the mean, also the variance of stimuli could influence the reproduction. Larger variance can be achieved by reducing the sampling frequency of the stimulus range or by expanding the width of the range, accommodating more distance time intervals. The effect of changing the variance of stimuli on the behavior has not been well studied. There are three different effects that greater variance could have on behavior. Reproductions could improve, leading to a weaker regression. This would mean that subjects

rely less on the prior. Intuitively, larger variance means that differences of time intervals get more apparent and discrimination becomes easier (e.g. stimuli are further apart or extremes are more distinct). This scenario is predicted by a model that uses noisy integrators linked by an adaptive reference in Thurley 2016. On the other hand, a change in variance might have no effect on behavior, if the mean is fixed. According to this, only the mean value would have an influence on the reproduction performance. This seems to be the case in Petzschner, Maier, et al. 2012, since performance of the range with larger variance doesn't get better. Finally, reproductions be worse with greater variance. This was demonstrated in the case of sound intensity estimations by Teghtsoonian and Teghtsoonian 1978. In most studies that included experimental data with varying variance of stimuli, the effects on regression were not examined.

6.2 Optimality Predicts Regression Effect and Range Effect

To test the behavior of the model with respect to the external variability of stimuli, additional ranges were used, differing in mean, width and sampling frequency. The short and the long range include seven stimuli spanning 300 ms, with mean values of 550 and 850 ms, respectively. Two ranges had the same variance and width, but shifted mean values at 700 ms (mid range) and 1050 ms (extra-long range). With increasing mean, the range effect predicts a flatter slope. In addition, ranges were examined whose mean was equal to one of the ranges above, but which had a higher variance. Including all stimuli from the short and the long range, the all range has the same mean as the mid range, but a larger width (600 ms) and therefore higher variance. The short-few and all-few range encompasses the short and the all range, respectively, but with smaller number of stimuli, the variance increases in both cases (Fig. 10a, Supplementary Fig. 7c). For all ranges, the slope of the linear regression between stimuli and reproductions is below one. Thus, simulations with error-minimizing parameters predict the regression effect across several ranges. The slopes decrease significantly as the mean of the stimulus range increases, except for the short and mid range (Fig. 10c). Thus, the model predicts the range effect only for sufficiently large changes in the mean. (Kolmogorov–Smirnov two-sample test, $p < 0.01$, $n=21$ for each distribution, Bonferroni correction for multiple testing). Across ranges that only change their mean value (short, mid, long and extralong), the slope has a linear correlation with the mean value of

the range (Pearson correlation $r=-0.95$, $p < 0.05$).

When the experiment was simulated with a common τ of 165 ms between ranges, K^* is significantly lower for the mid range (16.71) compared to the short range (21.33), but slopes show no significant difference (Supplementary Fig. 7a, b). Decreasing K^* for increasing mean of ranges is captured by the model beyond the short and the long range. (Kolmogorov–Smirnov two-sample test, $n=20$ for each distribution, $p<0.01$, Bonferroni correction for multiple testing).

What causes the range effect in the circuit model? The model is situated in a dynamic regime, that displays time reproductions close to real behavior. Error-minimizing parameters predict the regression and range effect across multiple stimulus ranges. Decreasing slopes for larger stimulus ranges occur because they approach the limit of the dynamic regime (Fig. 10b). When the stimulus ranges are pushed to more extreme values, the behavior of the model breaks down. Reasons for a breakdown of the behavior are a too large number of timeouts in the case too short time intervals. If time intervals are too, the variance in reproductions increases sharply and K is pushed to lower values, resulting in slopes that are outside the observed behavior. This means that the regime of the model has to be adapted to major changes in the external statistics.

6.3 Optimality Predicts no Effect of Variance on Behavior

How does the slope change when the mean of stimuli remains constant, but variance is increased? The statistics of stimuli can be summarized by the ratio of the mean and variance of the stimulus range: $\frac{E(t)}{\text{var}(t)}$. Higher variance in ranges with lower stimulus sampling (short-few, all-few) shows no significant difference from their counterparts with normal stimulus sampling (short, all). Furthermore, a larger width of stimuli does not result in a significant larger or smaller slope (all range vs mid range). Therefore, increasing variance is not affecting the reproduction of stimuli in the model. (Kolmogorov–Smirnov two-sample test, $n=21$ for each distribution, Bonferroni correction for multiple testing). Considering only the mean, there is a significant correlation with the slope (Pearson correlation $r=-0.96$, $p < 0.001$), but not with the external variability ratio (Pearson correlation $r=-0.65$, $p = 0.12$) (Fig. 10c). In the simulation with a common τ there is no significant difference in K^* when the variance is changed (Supplementary Fig. 7a, b). However, increasing the variance of a range leads to a significant increase in MSE in all cases (Fig. 10d). (Kolmogorov–Smirnov

two-sample test, $n=21$ for each distribution, $p<0.01$, Bonferroni correction for multiple testing).

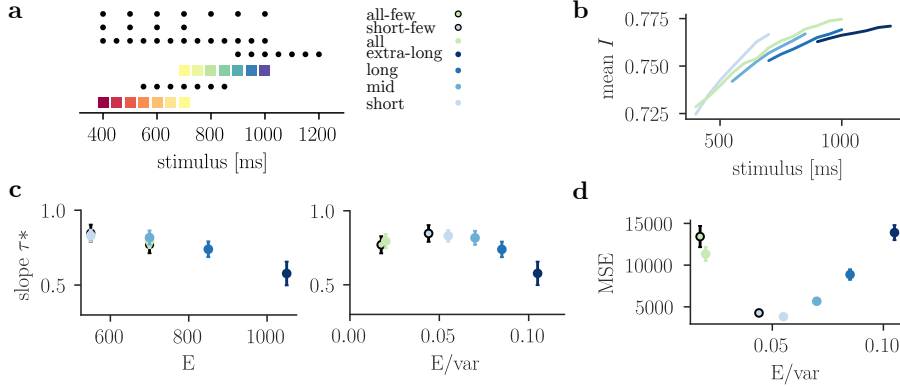


Figure 10: **Behavioral slopes with varying stimulus statistics.** (a) Parameter simulations were performed with stimulus ranges that differed in mean and variance to the short and long range. The mid range has its mean at the overlap of the short and long range. The extra-long range has its mean above the long range. Both the mid and extra-long range have the same number of stimuli (13) that spans the short and long range was included (all range). Both the short and the all range were for the short-few and all-few range under sampled. (b) Simulations were performed with optimized τ^* (and corresponding K^*): short 130 ms (14), mid 170 ms (17), long 200 ms (20), extra-long 230 ms (18), all 150 ms (14). Mean input I for each stimulus was calculated for stimulation with different ranges. Colors correspond to legend in (a). (c) Left: Slopes of behavioral results plotted against the mean of the range that was used. The error bars indicate standard deviation in the slope for different initialization. Colors correspond to legend in (a). Right: Slopes plotted against the ratio of the mean and the variance of each range. (d) The MSE for simulations with error-minimizing parameters, plotted against the ratio of mean and variance of the range.

6.4 Comparison of Behavioral Output of Model to Real Data

The circuit model predicts that a change in variance affects the MSE of the reproductions. It also predicts, that only the mean and not the variance has an effect on the regression of reproductions, which is in contrast to the noisy integrator model proposed by Thurley 2016. In the following section, we compare predictions of the model with behavioral data from time reproduction experiments with gerbils and humans. The stimuli in these experiments were several seconds long and came from either a short, mid, long or all range (data by Henke and Thurley).

Behavior in gebrils exhibits a regression effect for all ranges and a range effect for ranges with increasing mean. The variation in slopes between gebrils is considerably larger when the variance is increased. At the individual level, both consistent and increasing performance with increasing variance is observed. There are three gebrils that show a linear increase in performance with decreasing ratio of the mean and variance of the stimulus range (Fig. 11b). The remaining four gerbils however, show no effect of variance on reproductions (Supplementary Fig. 8a). On average Person correlation shows a significant linear relation of the slope with the mean ($r=-0.62, p < 0.001$) and ratio of mean and variance ($r=-0.61, p < 0.001$) in gerbils. This correlation gets stronger when the all range is excluded ($r=-0.75, p < 0.001$). In humans, behavior is heterogeneous, and there is no range effect on average, but there is in some individuals (Fig. 11). There is no significant correlations of the slope with the mean or external variability ratio. The root MSE increases as the variance increases across all subjects (Supplementary Fig. 8b).

The circuit model predicted no effect of variance on the regression, but on the error in reproductions. Gebrils show a discrepancy in performance when variance is increased. The model captures only one possible behavior, namely not taking into account a change in variance. There is no significant correlation of the slope with the external variability ratio in the model, when in gerbils there is. However, the model predicts correctly increasing error in reproductions with higher variance (Fig. 10b).

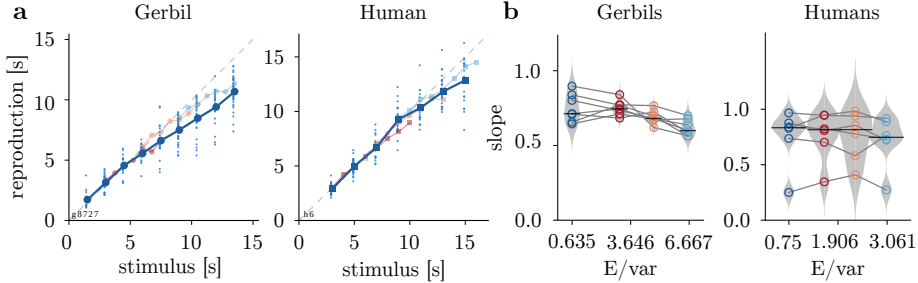


Figure 11: **Effects of stimuli statistics on behavior of gerbils and humans.** (a) Representative behavioral results of time reproduction of a gerbil (left) and a human (right). Stimuli were several seconds long. Four experiments were conducted with different ranges: short (red), mid (orange), long (light blue) and all (blue). Large markers display the mean of trials. Small dots show reproductions of single trials for the experiment with the all range. Ranges differed slightly between experiments with gerbils and humans. (b) Slope of the linear regression between stimuli and reproductions for seven gerbils (left) and six humans (right) plotted against the ratio of the mean and variance of the stimulus ranges. Vertical black markers indicate the median of slopes and gray violin plots illustrate the distribution over all animals. Slopes for different stimulus ranges of one animal are connected by lines. Figure courtesy of Kay Thurley and Josephine Henke.

7 Discussion

Previous results indicated, that time is encoded in dynamical changes of population activity, the rate of which is adjusted to the expected timing of movement initiation (Henke, Bunk, et al. 2021, Egger, Remington, et al. 2019, Remington et al. 2018, Wang et al. 2018). This led to the hypothesis, that control over timed behavior can be understood in terms of adjustments to initial conditions and external inputs of a dynamical system (Tsao et al. 2022, Remington et al. 2018, Wang et al. 2018). Further support was provided by the study of RNNs, that were trained on time reproduction tasks. When trained with a tonic input, RNNs generated smooth temporal scaling when exposed to novel inputs. This was not the case for RNNs trained on transient inputs, supporting the hypothesis of the speed-control mechanism via a tonic input (Zhou et al. 2022, Bi and Zhou 2020, Remington et al. 2018). The circuit model takes the core of this mechanism i.e. a dynamical systems approach and combines it with other evidence, like an action triggering state or an error signal, to facilitate time reproduction.

Speed control is implemented via a tonic input to two neurons, such that the readout unit scales its activity with the input and reaches a fixed threshold at different times, corresponding to the triggering of a response. The threshold corresponds to the action-triggering state in the population activity, when the

neural trajectory is projected onto the time axis Remington et al. 2018. In each trial, the model updates the input according to the stimulus interval. Previous work showed that the populations dynamics are sequentially updated based on an error signal to yield better estimates (Egger, Remington, et al. 2019). In the model, the error signal is extracted in the measurement epoch from the distance of the read-out activity to the threshold. The error is combined with a weight and used to either increase or decrease the input to match the time of threshold crossing to the stimulus interval in the reproduction. For judgments about time, the brain is thought to rely on an internal reference, that is sequentially updated over trials (Bausenhart et al. 2014, Dyjas et al. 2012). This concept is tightly connected to a Bayesian framework of magnitude estimation, where a prior is combined with current estimates (Petzschner, Glasauer, et al. 2015, Shi et al. 2013). In the circuit model, the input level in the measurement is inherited from the previous trial and updated before the reproduction epoch based on the weighted error. Thus, the inherited input to the measurement epoch is composed of the initial input and all past updates, which can be interpreted as a moving average of preceding inputs. The mean input over the course of an entire experiment reflects the prior or internal reference in the circuit model, corresponding to the mean stimulus interval. To better approximate the prior or internal reference hypothesis, the input in each measurement epoch could be set to a value equal to the moving average of the previous inputs, rather than being inherited from the previous trial. Taken together, the model uses the core elements that have been observed in data, but in a simplified way, making it possible to study the resulting dynamics in depth. It has already been shown that the model captures the classical effects of magnitude estimation when fitted to human data Egger, Le, et al. 2020.

Here, we extended the model to simulations of realistic time reproduction experiments that reflect stimulus variability by presenting random time intervals drawn from a stimulus distribution.

7.1 Representation of Stimulus Statistics

Simulations across a variety of stimulus ranges confirmed, that the model captures classical behavioral effects in realistic experiment settings under a parameter regime that minimizes errors in reproductions. This suggests, that adjusting neural dynamics based on an internal reference in the presence of noise could lead to the key effects found in time reproduction experiments such as the re-

gression effect, the range effect and scalar variability. Sohn et al. 2019 suggested that optimal integration of prior beliefs arise from the curved nature of neural trajectories. Based on the results from the circuit model, curvature of manifolds would not be necessary to achieve biases in the reproduction, as they result from a sequential weighted update of the speed command (external input), where the weight is adjusted based on the stimulus statistics.

Since the key effects of time estimation were reproduced in simulations, we tested additional parameters in the stimulus statistics, e.g. modifying the variance of the stimulus distribution, to test the model's behavior for different external variability. Only few studies have investigated an internal representation of temporal statistics. Acerbi et al. 2012 showed that humans are able to represent the statistics of stimulus distributions to the third moment in reproductions. However, the model did not predict an impact of the change in external variability on the regression effect, but did predict an impact on the error in reproductions. This finding was partially confirmed in gerbil data, but some animals differed from the group by accounting for the change in variance, as evidenced by an increase in performance of interval reproductions. Animals that considered the variance in the data seem to have adapted to the new stimulus statistics in contrast to the other animals. How neural dynamics adjusted to accommodate the new information provided by changed variance is still to be determined. Meirhaeghe et al. 2021 examined the adaptation to simultaneous changes in variance and mean of stimuli and identified modulations in the firing rates and adjusted speed in the population dynamic to take into account the new distribution mean. The influence of variance, however, was not investigated separately. Understanding how external stimulus statistics feed into the computations of timing in the brain can help us better understand the underlying mechanism. Further experiments should be conducted to investigate this shift to considering information from altered stimulus statistic. By gradually changing the variance the difference between animals in when and if adaptation occurs, could be revealed. Animals that did not increase performance in the present data might do so, if the variance is further increased. Based on new evidence, the model would need to be extended to account for this adaptation in dynamics that improves performance.

7.2 Scales of Timing

Timing encompasses various scales, ranging from microseconds, milliseconds, seconds to circadian rhythms. This raises the question of how timing mechanisms can accommodate time computations for widely spaced intervals. While circadian rhythms rely on distinct mechanisms to encode time, it is not clear whether there are different timing mechanisms between subsecond and suprasecond (Tsao et al. 2022, Paton and Buonomano 2018, Buonomano 2007, Buonomano and Karmarkar 2002). Neural trajectories encoding time have been identified in both the subsecond (Meirhaeghe et al. 2021, Sohn et al. 2019) and suprasecond scale (Henke, Bunk, et al. 2021), though adaptations of dynamics seem to take place. This becomes apparent when comparing the regression effect between experiments conducted with ranges in different timescales. The range effect does not propagate from the subsecond scale to ranges in the suprasecond scale, in other words, the slopes for regression are independent and start close to 1 for short ranges in the suprasecond scale.

Simulations with the circuit model revealed that there is a limited regime in which the model exhibits the classical magnitude estimation effects. For stimulus ranges that are much larger or smaller than those we used, the behavior of the model breaks down. This means that when the model is used in experiments with even shorter or longer time intervals, the operating regime of the model must be adjusted to accommodate for the new timescale. To return to the model implementation: No statement is made about the timescale. Rather, the scale is set arbitrarily from the outside by assigning a unit to the time bins. Thus, the model's operating regime can be moved to other timescales by resealing the time axis, which is equivalent to changing the units of time bins.

How the adaptation to different timescales is realized in terms of neural trajectories is unknown. A different form of adaptation of neural trajectories to experiment setting has been shown by Remington et al. 2018. In experiments that involved a gain in reproductions, they identified a flexible displacement of neural trajectories in the state space. Further experiments need to investigate if a displacement of neural trajectories could explain an adaptation to new timescales. It must be clarified whether this adaptation to the timescale is gradual or immediate. Further work on the model will need to figure out how to incorporate this adaptation to timescales into the model, rather than imposing it externally.

7.3 Integration into Classical and Bayesian Framework

Classical models of timing can be categorized in two main classes. Dedicated models rely on specialized and centralized mechanisms, including oscillator models and pacemaker-accumulator models that produce ramping activity in single cells. Intrinsic models are based on local and general properties of neural circuits, comprising ramping models and state-dependent network models (Paton and Buonomano 2018, Goel and Buonomano 2014). The circuit model distinguishes itself from classical timing models because it is situated on a mechanistic level. It produces ramping behavior by interactions of neurons and allows for flexible behavior by adjusting to sensory feedback (Egger, Le, et al. 2020). It is important to point out, that this model does not depend on an internal pacemaker to track time, since time is encoded in changes of neural dynamics. A link between the circuit model and the main classes of timing models has already been made in Egger, Le, et al. 2020.

A statistical approach that is often used to explain effects in timing behavior is the Bayesian framework (Sohn et al. 2019, Petzschner, Glasauer, et al. 2015 Shi et al. 2013 Petzschner, Maier, et al. 2012). While perceptual systems might be Bayesian at the computational level, they are probably not at the algorithmic and implementation level (Block 2018, Kwisthout and Rooij 2020, Marr and Poggio 1977). The circuit model is situated at the algorithmic level, possibly providing an algorithmic implementation of the Bayesian framework. The input to the model in the measurement epoch represents prior information about previous trials. Based on this prior information, the simulation period yields an error signal that is dependent on the current stimulus interval. With a weighted update of the input, prior information is combined with current sensory information. This way the estimate in the reproduction epoch is accomplished. The weight depends on the external variability, i.e. length of time intervals.

The circuit model is able to link neural activity to behavior and explains the key effects of magnitude estimation by combining prior information with a weighted error signal. Certainly, there are more factors like non-temporal context e.g. intensity effects or sensory modality differences that are not captured by the model. This work, however, provided further evidence that a dynamical systems perspective has the potential to explain flexible timing.

Supplements

Methods

Circuit

For simulating the dynamics of u , v , y and I Euler's method was used with a step size Δt set to 10 ms. The reset mechanism of u and v is switched on for one time step after every epoch and the update mechanism of I is switched on for one time step after the measurement epoch only. Noise is independently sampled for every time step from a Gaussian distribution with standard deviation σ .

Timeouts

Reproductions that do not reach the threshold in a certain time span (twice the stimulus interval) are classified as timeout trials. If the threshold is crossed particularly early, the trial is also classified as (early) timeout trial (crossing before 0.2 of stimulus interval). Simulations that exceed a fixed number of timeout trials (10% of all trials in the experiment) were excluded from analysis. If timeout trials occurred for a single stimulus more than 10% of all trials of this stimulus, the simulation was also discharged. For different parameter combinations, the number of timeouts were exceeded (a combination of too small τ and too high K).

Experiment Simulation

In all simulations in the intermediate regime, the threshold y_{th} was set to 0.7. The model worked with higher and lower thresholds robustly. For experiment simulations with 500 trials, the increase of the standard deviation of reproductions plateaus with noise levels $\sigma > 0.1$. This was tested with parameters set to $\tau = 100$, $K_{\text{short}} = 8.5$ and $K_{\text{long}} = 6$. The standard deviation of reproductions grows monotonically for increasing stimulus intervals for tested noise levels (Supplementary Fig. 1b). Further, the coefficient of variation (CV) was used to quantify the degree of variation. It is defined as $\text{CV} = \frac{\sigma_{\text{reproduction}}}{\mu}$ for each stimulus, where μ corresponds to the stimulus interval and $\sigma_{\text{reproduction}}$ to the standard deviation of the corresponding reproductions. To achieve variations close to real data, reproductions should have a CV of 0.2 to 0.4 that is constant over all stimulus intervals (Supplementary Fig. 1c). For all simulations the

noise level σ was set to 0.02, where the mean CV for the short range was 0.1 and for the long range 0.15 with the parameters from above.

In all experiment simulations, a series of 500 trials was presented to the model. Stimuli were randomly chosen from the short (400-700 ms) or the long (700-1000 ms) stimulus range (Supplementary Fig. 1a). The stimulus series had a uniform distribution of stimuli, a repetition of all seven stimuli in every 20 trial windows and no remarkable oscillation. To allow for optimization of K the same stimulus series was used. Added noise was initialized equally to extract changes in results only based on parameter changes. Different noise initialization influence the optimal value of K slightly. For 20 simulations with $\tau = 140$ and $\sigma = 0.02$ the mean optimal K and standard deviation for the short range were $K = 14.45$, std = 0.49 and for the long range $K = 9.91$, std = 0.77.

Optimality by Minimizing MSE

We minimized the error in the interval reproductions across the experiment, we defined the $MSE = \text{bias}^2 + \text{var}$, with the bias specified as the squared difference between the mean reproduction \bar{t}_r for each stimulus interval t_s in the stimulus range S and variance as mean σ^2 for all stimulus intervals in S .

$$\begin{aligned}\text{bias} &= \frac{1}{S} \sum_{i=1}^S (\bar{t}_{r_i} - t_{s_i}) , \\ \text{bias}^2 &= \frac{1}{S} \sum_{i=1}^S (\bar{t}_{r_i} - t_{s_i})^2 , \\ \text{var} &= \frac{1}{S} \sum_{i=1}^S (\sigma_i^2) .\end{aligned}\tag{1}$$

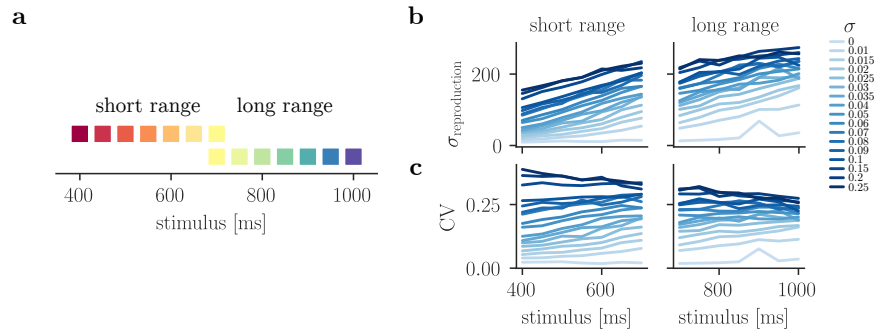
Errors Minimization with Other Metrics

Optimal values of K are based on the MSE, which composed of the squared bias and the variance of reproductions. Time constants τ with the minimal MSE for a value of K differ between the short and the long range. For the short range the optimal time constant $\tau = 120ms$, for the long range $\tau = 200ms$ (Supplementary Fig. 3a, b). If optimization is based only on the squared bias, optimal time constants are 100 ms for the short and 110 ms for the long range. The variance is pushing the optimal time constant to larger values for both stimulus ranges. Similarly, optimal K is pushed to lower values by the variance (Supplementary

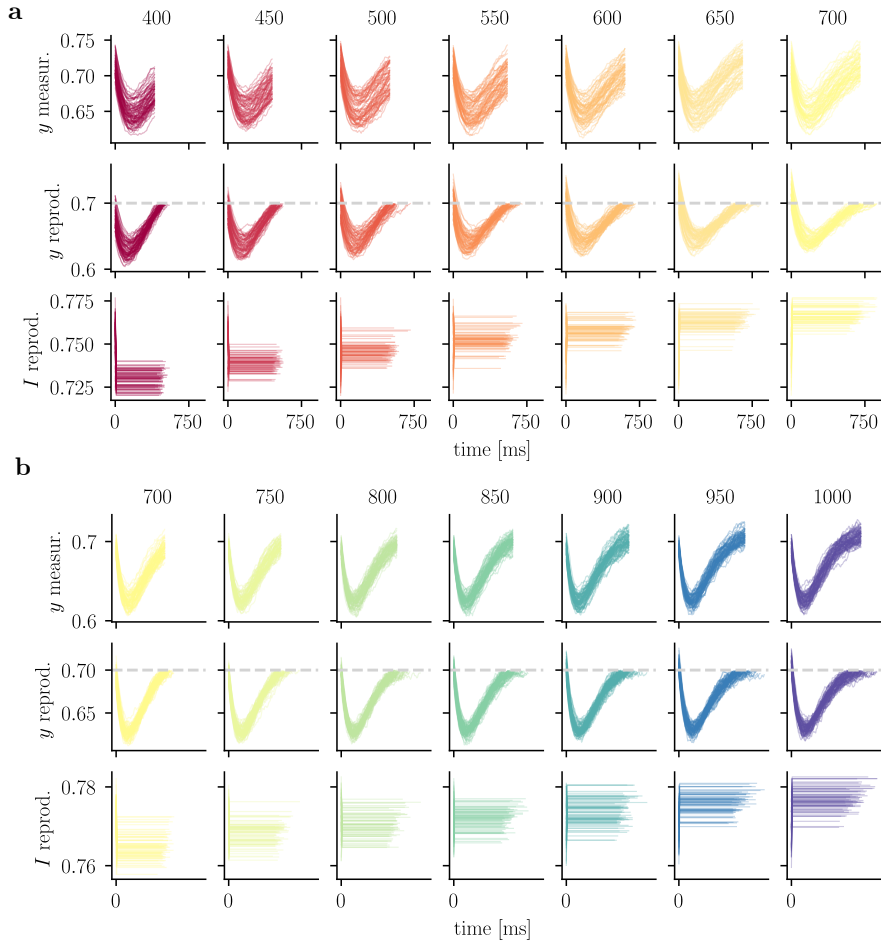
Fig. 3c, d). For all optimized values, be it on the squared bias, the variance or combined in the MSE, there is a general underestimation of stimulus intervals from the long range, which becomes appeared in Supplementary Fig. 3e.

Statistical Analysis

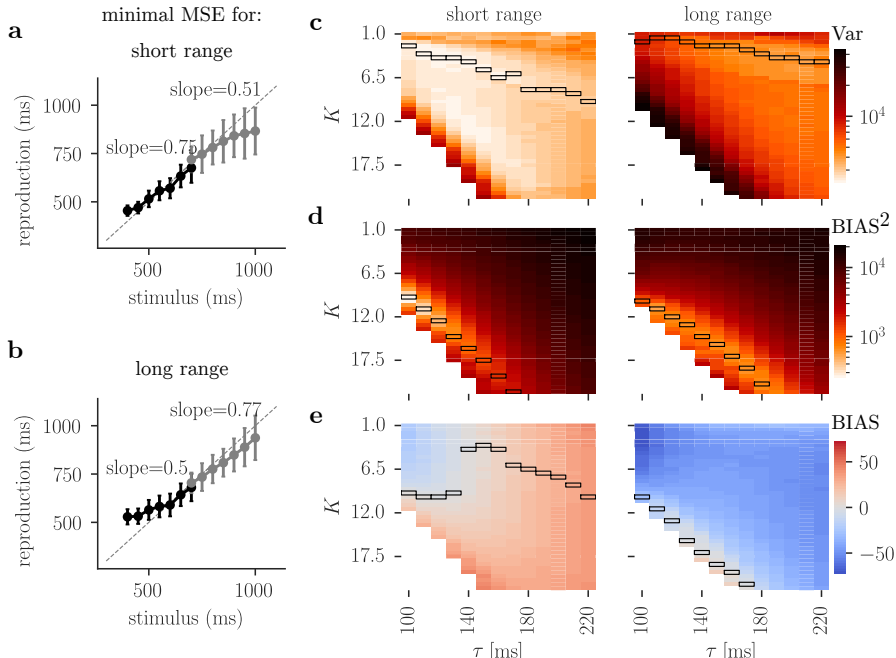
Supplementary Figures



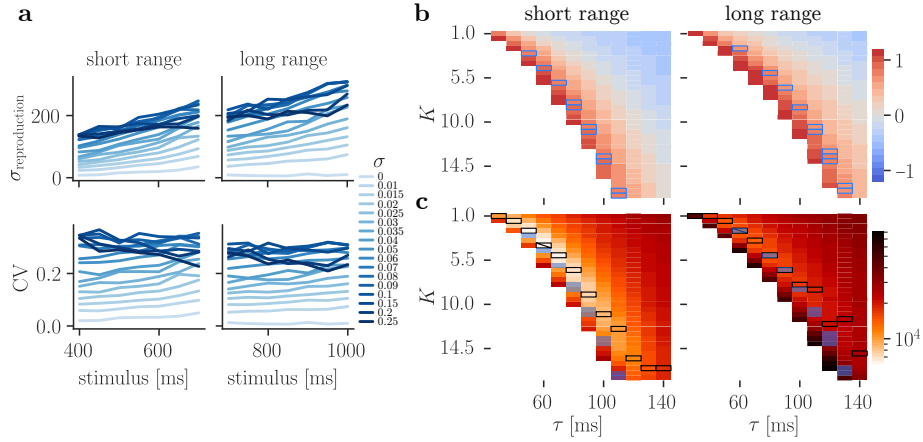
Supplementary Figure 1: **Experiment description and noise levels.** (a) The short and the long stimulus range comprised time intervals from 400 to 700 ms and 700 to 1000 ms, respectively. (b) Standard deviation of reproductions for each stimulus in an experiment simulation with 500 trials and $\tau = 100$. K was set to 8.5 and 6 for the short and long range respectively. (c) Same as (a) but standard deviation of reproductions normalized by stimulus duration (CV).



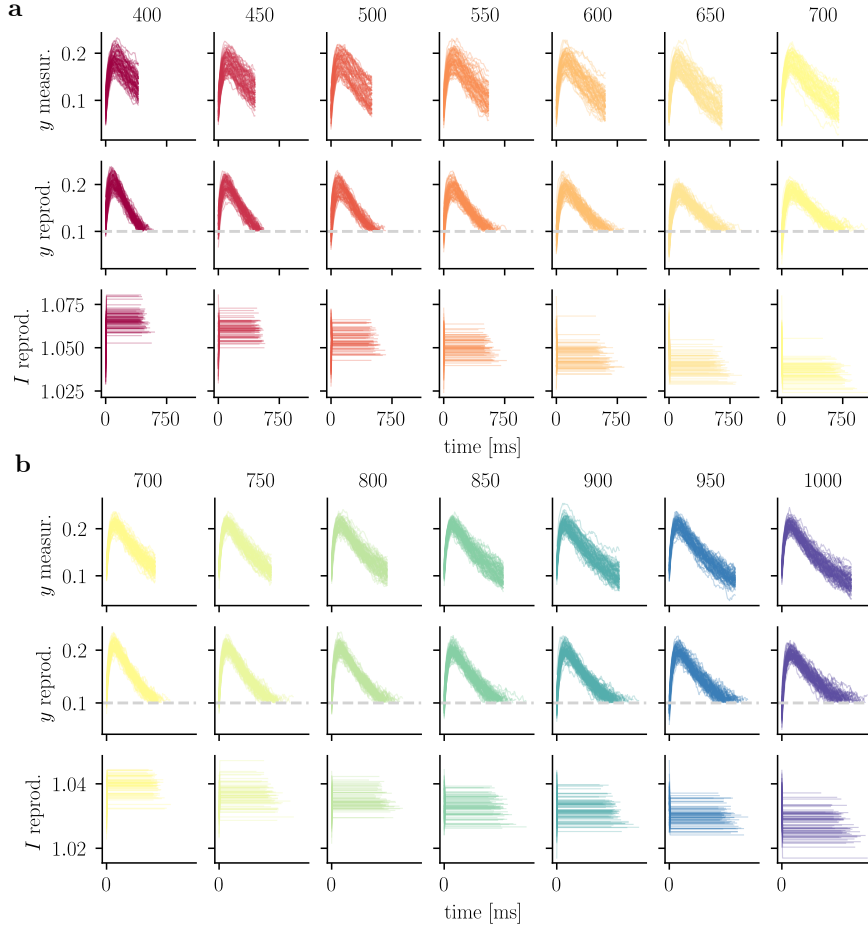
Supplementary Figure 2: **Experiment dynamics with optimized K .** (a) For an experiment simulation with 500 trials, a time constant τ of 130 and optimal $K = 13$, the activity was sorted according to epoch and stimulus interval. Stimuli were chosen from the short range. Upper row show the behavior of y in the measurement epoch, middle row shows the behavior of y in the reproduction epoch. The lower row shows the input level to the circuit during the reproduction epoch. (b) Same as (a) with stimuli chosen from the long range and $K = 10$.



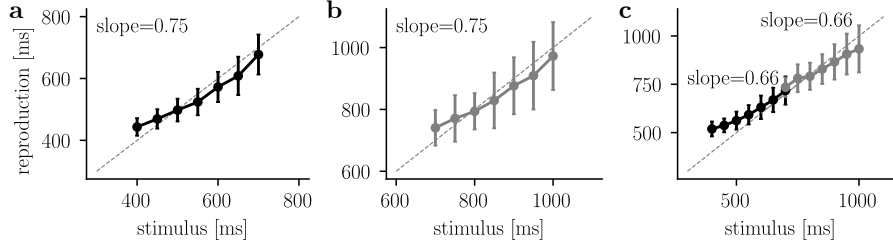
Supplementary Figure 3: **Extended parameter optimization.** (a) Behavioral results for a simulation with 500 trials, $\sigma = 0.02$ and optimized time constant τ for the short range ($\tau = 120$). For simulations with both short and long range, the optimal time constant for the short range was used. Optimal K for $\tau = 120$ was 11 for the short, 7 for the long range. (b) Same as (a) with optimized τ for the long range ($\tau = 200$). Optimal K for this time constant was 25 for the short range and 20 for the long range. (c) Simulations with 500 trials for each pair of memory parameter K , and τ at noise level $\sigma = 0.02$. Simulations were performed with stimuli chosen from the short (left) or long range (right). Color scale represents the variance of reproductions in the behavioral results. Minimal variance for each τ is encircled. (d) Same as (c), color scale represents the squared bias of reproductions. Minimal squared bias for each τ is encircled. (e) Same as (d), color scale represents the bias of reproductions. Values larger than 0 correspond to an overestimation, values smaller than 0 to an underestimation of the stimulus interval. Bias closest to 0 for each τ is encircled.



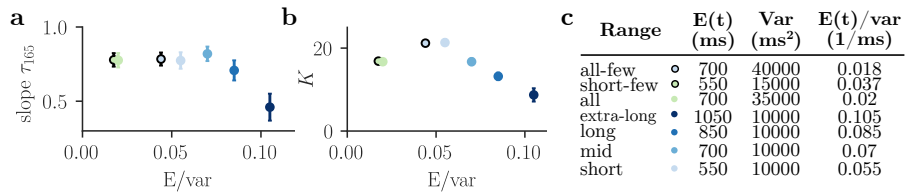
Supplementary Figure 4: Experiment description and parameter optimization in the high input regime. (a) Evaluation of noise for the high input regime of the model. Standard deviation (upper) and CV (lower) of reproductions for each stimulus in an experiment simulation with 500 trials and $\tau = 70$. K was set to 6 and 4 for the short and long range, respectively. (b) Simulations with 500 trials for each pair of memory parameter K and time constant τ at noise level $\sigma = 0.02$. Simulations were performed with stimuli chosen from the short (left) or long range (right). Color scale represents the slope of the linear fit between stimuli and reproductions. Behaviorally plausible slopes are encircled in blue and lie around 0.83 for the short and 0.73 for the long range. Empty spaces show simulations, that exceeded the number of timeout trials and where thus excluded from analysis. (c) Optimization of the memory parameter K in the high input regime for different time constants τ at noise level $\sigma = 0.02$. Color scale represents the MSE for an experiment stimulation with 500 trials for each pair of K and τ . Stimuli were either chosen from the short (left) or the long stimulus range. The minimal error for each τ is encircled in black and minimal error across all τ is additionally crossed. Parameter combinations that result in behavioral plausible slopes (b) are shaded in blue.



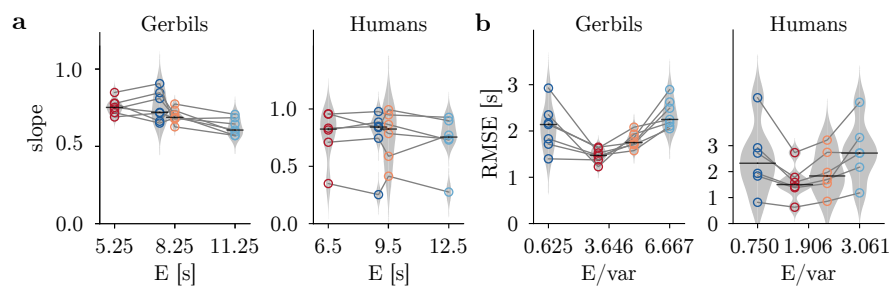
Supplementary Figure 5: **Experiment dynamics in the high input regime.** (a) For an experiment simulation with 500 trials in the high input regime. The threshold is set to $y_{\text{th}} = 0.1$ and $\sigma = 0.02$. Parameters are set to optimized values with time constant $\tau = 60$ and $K = 4$. The activity was sorted according to epoch and stimulus interval. Stimuli were chosen from the short range. Upper row show the behavior of y in the measurement epoch, middle row shows the behavior of y in the reproduction epoch. The lower row shows the input level to the circuit during the reproduction epoch. (b) Same as (a) with stimuli chosen from the long range and $K = 2.5$.



Supplementary Figure 6: **Behavioral results with different delay periods.** (a) Behavioral results of an experiment simulation with stimuli of the short range and the delay period set to the mean of short range (550 ms). Time constant and update parameter are optimized based by minimizing the MSE ($\tau = 130$, $K = 13$). Other parameters like σ , threshold and initial values were not changed compared to previous simulations. (b) Same as (a) but for the long range with the delay period set to mean of the long range (850 ms). Optimized $\tau = 220$ and $K = 22$. (c) Behavioral results of experiment simulation with both the long and the short range and the delay period set to 1000 ms. The time constant is set 160 ms, which corresponds to the mean of the optimal τ for the short (110 ms) and long (210 ms) range. Optimal K for the short ($K = 17$) and long ($K = 11$) range is optimized for the chosen time constant.



Supplementary Figure 7: **Influence of external variability on behavior with shared time constant.** (a) The slope of behavior resulting from experiment simulations with optimized K for different ranges was determined and plotted against the ratio of mean and variance of the stimulus range. The time constant was set to 165 ms for all ranges, which corresponds to the mean of the optimal time constant of the short and long range. The error bars indicate standard deviation in the slope for different initialization. Colors correspond to the legend in (c). (b) K that minimized errors for a time constant of 165 ms for all ranges. K is plotted against the ratio mean and the variance of the stimulus range. The error bars indicate standard deviation in the slope for different initialization. (c) Overview of all ranges used for simulations with their mean, variance and the ratio of both, that is used to characterize the ranges.



Supplementary Figure 8: **Effects of stimuli statistics on behavior of gerbils and humans.** (a) Slope of the linear regression between stimuli and reproductions for seven gerbils (left) and six humans (right) plotted against the mean of the stimulus ranges. Vertical black markers indicate the median of slopes and gray violin plots illustrate the distribution over all animals. Slopes for different stimulus ranges of one animal are connected by lines. Note that ranges short (red), mid (orange), long (light blue) and all (blue) differed slightly between experiments with gerbils and humans. (b) xxx Figure courtesy of Kay Thurley and Josephine Henke.

Code

Design

The code is designed in a modular way, such that multiple types of experimental procedures with shared functionality are accessing the same basic circuit, which is implemented in `BaseSimulation` as shown in Figure 9. The implementation of the basic circuit can be reused for all epochs. Different experiments can have different result types, all of which can be found in `result.py`. After each experiment, the results are gathered and stored together, consisting of the parameter set, the simulation time course, a list of reset time points, a list of production times, a list of indices of timeout trials and the stimulus list. Analysis of the results is performed in the same file. Depending on the analysis (e.g. behavioral), different plots are implemented in `plot.py` to visualize the results.

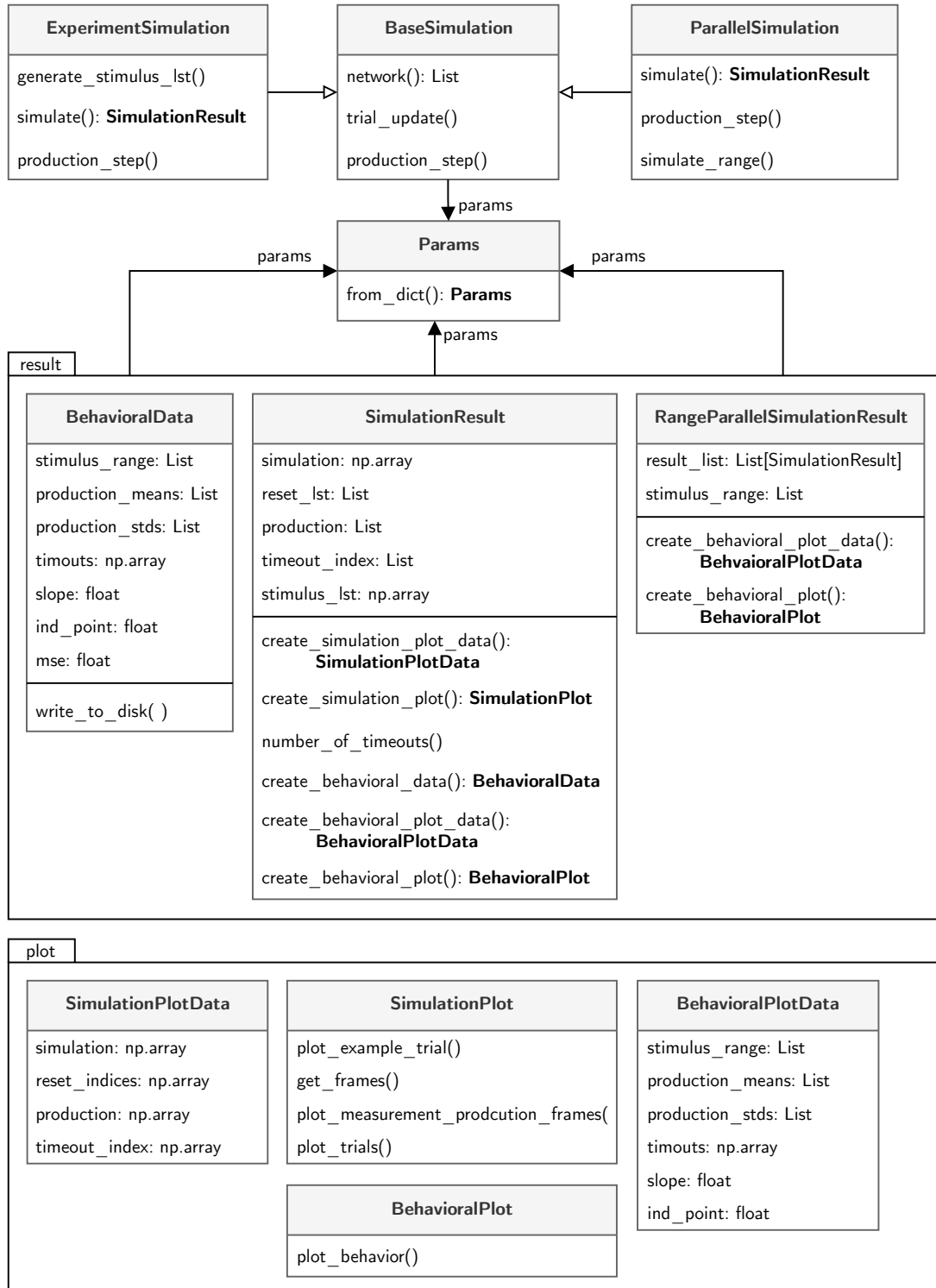
All parameters are set and described in `Params` and can be modified individually or by reading a parameter dictionary. The parameters configure the circuit. To initiate a simulation, the parameter set is handed to one of the implemented experiments. An interval reproduction experiment, as described in this report is implemented in `experiment_simulation.py`. Parallel simulations of one trial (one delay, measurement and reproduction epoch) is implemented in `parallel_simulation.py`. Both `experiment_simulation.py` and `parallel_simulation.py` contain a `simulate` function that accesses the base simulation (`BaseSimulation`) with the implementation of the basic circuit. For each epoch or update/reset step, the `simulate` function feeds the according time steps and initial conditions into the network in `BaseSimulation`. Depending on the epoch, the reset and update mechanism are tuned on or off. After each epoch or pulse, the results of the network are joint to the time course of the experiment in `trial_update`. The `simulate` function returns a `SimulationResult` or `RangeParallelSimulationResult` object.

For an overview of the code structure see Figure 9 and for its usage see `simulations.ipynb` at github.com/KatharinaBracher/MScThesis.

Implementation

All simulations and analysis were performed with Python 3.9.7. The following libraries were used: `matplotlib` (3.5.1), `NumPy` (1.22.3), `SciPy` (1.8.0), `scikit-learn` (1.0.2). An experiment simulation can not be parallelized, since each step

depends on the previous one.



Supplementary Figure 9: **Design.** The base simulation and different procedures (experiment, parallel) are all implemented in separate files. All results and analysis are collected in `result.py`, all plot for different result types are collected in `plot.py`

References

- Acerbi, Luigi, Daniel M. Wolpert, and Sethu Vijayakumar (2012). “Internal Representations of Temporal Statistics and Feedback Calibrate Motor-Sensory Interval Timing”. *PLoS Computational Biology* 8.11. ISSN: 15537358. DOI: 10.1371/journal.pcbi.1002771.
- Bausenhart, Karin M., Oliver Dyjas, and Rolf Ulrich (Mar. 2014). “Temporal reproductions are influenced by an internal reference: Explaining the Vierordt effect”. *Acta Psychologica* 147, pp. 60–67. ISSN: 00016918. DOI: 10.1016/j.actpsy.2013.06.011.
- Bi, Zedong and Changsong Zhou (2020). “Understanding the computation of time using neural network models”. *Proceedings of the National Academy of Sciences of the United States of America* 117.19, pp. 10530–10540. ISSN: 10916490. DOI: 10.1073/pnas.1921609117. arXiv: 1910.05546.
- Block, Ned (Sept. 2018). *If perception is probabilistic, why does it not seem probabilistic?* DOI: 10.1098/rstb.2017.0341.
- Bubic, Andreja, D. Yves von Cramon, and Ricarda I. Schubotz (2010). “Prediction, cognition and the brain”. *Frontiers in Human Neuroscience* 4.March, pp. 1–15. ISSN: 16625161. DOI: 10.3389/fnhum.2010.00025.
- Buonomano, Dean V. (Oct. 2007). *The biology of time across different scales*. DOI: 10.1038/nchembio1007-594.
- Buonomano, Dean V. and Uma R. Karmarkar (June 2002). *How do we tell time?* DOI: 10.1177/107385840200800109.
- Cicchini, Guido Marco, Roberto Arrighi, Luca Cecchetti, Marco Giusti, and David C. Burr (Jan. 2012). “Optimal encoding of interval timing in expert percussionists”. *Journal of Neuroscience* 32.3, pp. 1056–1060. ISSN: 02706474. DOI: 10.1523/JNEUROSCI.3411-11.2012.
- Clark, Andy (2013). “Whatever next? Predictive brains, situated agents, and the future of cognitive science”. *Behavioral and Brain Sciences* 36.3, pp. 181–204. ISSN: 14691825. DOI: 10.1017/S0140525X12000477.
- Cueva, Christopher J., Alex Saez, Encarni Marcos, Aldo Genovesio, Mehrdad Jazayeri, Ranulfo Romo, C. Daniel Salzman, Michael N. Shadlen, and Stefano Fusi (Sept. 2020). “Low-dimensional dynamics for working memory and time encoding”. *Proceedings of the National Academy of Sciences of the United States of America* 117.37, pp. 23021–23032. ISSN: 10916490. DOI: 10.1073/pnas.1915984117.

- Dyjas, Oliver, Karin M. Bausenhart, and Rolf Ulrich (2012). “Trial-by-trial updating of an internal reference in discrimination tasks: Evidence from effects of stimulus order and trial sequence”. *Attention, Perception, and Psychophysics* 74.8, pp. 1819–1841. ISSN: 19433921. DOI: 10.3758/s13414-012-0362-4.
- Egger, Seth W., Nhat M. Le, and Mehrdad Jazayeri (2020). “A neural circuit model for human sensorimotor timing”. *Nature Communications* 11.1, pp. 1–14. ISSN: 20411723. DOI: 10.1038/s41467-020-16999-8.
- Egger, Seth W., Evan D. Remington, Chia Jung Chang, and Mehrdad Jazayeri (2019). “Internal models of sensorimotor integration regulate cortical dynamics”. *Nature Neuroscience* 22.11, pp. 1871–1882. ISSN: 15461726. DOI: 10.1038/s41593-019-0500-6.
- Emmons, Eric B., Benjamin J. De Corte, Youngcho Kim, Krystal L. Parker, Matthew S. Matell, and Nandakumar S. Narayanan (Sept. 2017). “Rodent medial frontal control of temporal processing in the dorsomedial striatum”. *Journal of Neuroscience* 37.36, pp. 8718–8733. ISSN: 15292401. DOI: 10.1523/JNEUROSCI.1376-17.2017.
- Ficco, Linda, Lorenzo Mancuso, Jordi Manuello, Alessia Teneggi, Donato Liloia, Sergio Duca, Tommaso Costa, Gyula Zoltán Kovacs, and Franco Cauda (Dec. 2021). “Disentangling predictive processing in the brain: a meta-analytic study in favour of a predictive network”. *Scientific Reports* 11.1, pp. 1–14. ISSN: 20452322. DOI: 10.1038/s41598-021-95603-5.
- Genovesio, Aldo, Satoshi Tsujimoto, and Steven P. Wise (May 2006). “Neuronal Activity Related to Elapsed Time in Prefrontal Cortex”. *Journal of Neurophysiology* 95.5, pp. 3281–3285. ISSN: 0022-3077. DOI: 10.1152/jn.01011.2005.
- Goel, Anubhuti and Dean V. Buonomano (2014). “Timing as an intrinsic property of neural networks: Evidence from in vivo and in vitro experiments”. *Philosophical Transactions of the Royal Society B: Biological Sciences* 369.1637. ISSN: 09628436. DOI: 10.1098/rstb.2012.0460.
- Henke, Josephine, David Bunk, Dina von Werder, Stefan Häusler, Virginia L. Flanagin, and Kay Thurley (2021). “Distributed coding of duration in rodent prefrontal cortex during time reproduction”. *eLife* 10, pp. 1–24. ISSN: 2050084X. DOI: 10.7554/eLife.71612.
- Henke, Josphine, Virginia L. Flanagin, and Kay Thurley (Aug. 2022). “A virtual reality time reproduction task for rodents”. *Frontiers in Behavioral Neuroscience* 16. ISSN: 16625153. DOI: 10.3389/fnbeh.2022.957804.

- Huang, Yanping and Rajesh P.N. Rao (Sept. 2011). *Predictive coding*. DOI: 10.1002/wcs.142.
- Issa, John B, Gilad Tocker, Michael E Hasselmo, James G Heys, and Daniel A Dombeck (2020). “Navigating Through Time: A Spatial Navigation Perspective on How the Brain May Encode Time”. DOI: 10.1146/annurev-neuro-101419.
- Jazayeri, Mehrdad and Michael N. Shadlen (Aug. 2010). “Temporal context calibrates interval timing”. *Nature Neuroscience* 13.8, pp. 1020–1026. ISSN: 10976256. DOI: 10.1038/nn.2590.
- Kwisthout, Johan and Iris van Rooij (June 2020). “Computational Resource Demands of a Predictive Bayesian Brain”. *Computational Brain and Behavior* 3.2, pp. 174–188. ISSN: 2522087X. DOI: 10.1007/s42113-019-00032-3.
- Lewis, P. A., A. M. Wing, P. A. Pope, P. Praamstra, and R. C. Miall (2004). “Brain activity correlates differentially with increasing temporal complexity of rhythms during initialisation, synchronisation, and continuation phases of paced finger tapping”. *Neuropsychologia* 42.10, pp. 1301–1312. ISSN: 00283932. DOI: 10.1016/j.neuropsychologia.2004.03.001.
- Marr, D. C. and T. Poggio (May 1977). “From understanding computation to understanding neural circuitry”. *Neurosciences Research Program Bulletin* 15.3, pp. 470–488. ISSN: 00283967.
- Meirhaeghe, Nicolas, Hansem Sohn, and Mehrdad Jazayeri (2021). “A precise and adaptive neural mechanism for predictive temporal processing in the frontal cortex”. *Neuron* 109.18, 2995–3011.e5. ISSN: 10974199. DOI: 10.1016/j.neuron.2021.08.025.
- Mita, Akihisa, Hajime Mushiake, Keisetsu Shima, Yoshiya Matsuzaka, and Jun Tanji (2009). “Interval time coding by neurons in the presupplementary and supplementary motor areas”. *Nature Neuroscience* 12.4, pp. 502–507. ISSN: 10976256. DOI: 10.1038/nn.2272.
- Murakami, Masayoshi, M. Inês Vicente, Gil M. Costa, and Zachary F. Mainen (2014). “Neural antecedents of self-initiated actions in secondary motor cortex”. *Nature Neuroscience* 17.11, pp. 1574–1582. ISSN: 15461726. DOI: 10.1038/nn.3826.
- Paton, Joseph J. and Dean V. Buonomano (2018). “The Neural Basis of Timing: Distributed Mechanisms for Diverse Functions”. *Neuron* 98.4, pp. 687–705. ISSN: 10974199. DOI: 10.1016/j.neuron.2018.03.045.
- Petzschner, Frederike H., Stefan Glasauer, and Klaas E. Stephan (2015). “A Bayesian perspective on magnitude estimation”. *Trends in Cognitive Sci-*

- ences* 19.5, pp. 285–293. ISSN: 1879307X. DOI: 10.1016/j.tics.2015.03.002.
- Petzschner, Frederike H., Paul Maier, and Stefan Glasauer (July 2012). “Combining symbolic cues with sensory input and prior experience in an iterative Bayesian framework”. *Frontiers in Integrative Neuroscience* JULY 2012. ISSN: 16625145. DOI: 10.3389/fnint.2012.00058.
- Rao, Rajesh P.N. and Dana H. Ballard (Jan. 1999). “Predictive coding in the visual cortex: A functional interpretation of some extra-classical receptive-field effects”. *Nature Neuroscience* 2.1, pp. 79–87. ISSN: 10976256. DOI: 10.1038/4580.
- Remington, Evan D., Devika Narain, Eghbal A. Hosseini, and Mehrdad Jazayeri (June 2018). “Flexible Sensorimotor Computations through Rapid Reconfiguration of Cortical Dynamics”. *Neuron* 98.5, 1005–1019.e5. ISSN: 10974199. DOI: 10.1016/j.neuron.2018.05.020.
- Roxin, Alex and Anders Ledberg (Mar. 2008). “Neurobiological Models of Two-Choice Decision Making Can Be Reduced to a One-Dimensional Nonlinear Diffusion Equation”. *PLoS Computational Biology* 4.3. Ed. by Lyle J. Graham, e1000046. ISSN: 1553-7358. DOI: 10.1371/journal.pcbi.1000046.
- Shi, Zhuanghua, Russell M. Church, and Warren H. Meck (Nov. 2013). *Bayesian optimization of time perception*. DOI: 10.1016/j.tics.2013.09.009.
- Shima, Keisetsu and Jun Tanji (2000). “Neuronal activity in the supplementary and presupplementary motor areas for temporal organization of multiple movements”. *Journal of Neurophysiology* 84.4, pp. 2148–2160. ISSN: 00223077. DOI: 10.1152/jn.2000.84.4.2148.
- Sohn, Hansem, Devika Narain, Nicolas Meirhaeghe, and Mehrdad Jazayeri (2019). “Bayesian Computation through Cortical Latent Dynamics”. *Neuron* 103.5, 934–947.e5. ISSN: 10974199. DOI: 10.1016/j.neuron.2019.06.012.
- Straka, Hans, John Simmers, and Boris P. Chagnaud (2018). “A New Perspective on Predictive Motor Signaling”. *Current Biology* 28.5, R232–R243. ISSN: 09609822. DOI: 10.1016/j.cub.2018.01.033.
- Teghtsoonian, Robert and Martha Teghtsoonian (1978). *Range and regression effects in magnitude scaling*. Tech. rep. 4. Northampton, pp. 305–314. DOI: <https://doi.org/10.3758/BF03204247>.
- Thurley, Kay (2016). “Magnitude estimation with noisy integrators linked by an adaptive reference”. *Frontiers in Integrative Neuroscience* 10.FEB2016, pp. 1–11. ISSN: 16625145. DOI: 10.3389/fnint.2016.00006.

- Thurley, Kay and Ulrike Schild (Dec. 2018). “Time and distance estimation in children using an egocentric navigation task”. *Scientific Reports* 8.1, p. 18001. ISSN: 20452322. DOI: 10.1038/s41598-018-36234-1.
- Tsao, Albert, S. Aryana Yousefzadeh, Warren H. Meck, May Britt Moser, and Edvard I. Moser (Nov. 2022). *The neural bases for timing of durations*. DOI: 10.1038/s41583-022-00623-3.
- Wang, Jing, Devika Narain, Eghbal A. Hosseini, and Mehrdad Jazayeri (2018). “Flexible timing by temporal scaling of cortical responses”. *Nature Neuroscience* 21.1, pp. 102–112. ISSN: 15461726. DOI: 10.1038/s41593-017-0028-6.
- Xu, Min, Si Yu Zhang, Yang Dan, and Mu Ming Poo (Jan. 2014). “Representation of interval timing by temporally scalable firing patterns in rat prefrontal cortex”. *Proceedings of the National Academy of Sciences of the United States of America* 111.1, pp. 480–485. ISSN: 00278424. DOI: 10.1073/pnas.1321314111.
- Zhou, Shanglin, Sotiris C. Masmanidis, and Dean V. Buonomano (2022). “Encoding time in neural dynamic regimes with distinct computational trade-offs”. *PLoS Computational Biology* 18.3, pp. 1–29. ISSN: 15537358. DOI: 10.1371/journal.pcbi.1009271.